DNA damage and the *Trypanosoma brucei* cell cycle.

Glynn Robert Forsythe

Submitted in fulfilment of the requirements for the Degree of Master of Science

Institute of Infection, Immunity and Inflammation
College of Medical, Veterinary and Life Sciences
University of Glasgow

Abstract

Trypanosoma brucei demonstrates unique features in its cell cycle and response to DNA damage, two aspects of biology which are intricately linked. Here, a technique for producing populations of bloodstream form parasites synchronised in S phase is developed and attempts made to use this technique to search for cell cycle linked changes in the levels of DNA damage response proteins. Additionally, two proteins central to the control of the DNA damage response in other organisms, ATM and ATR, are analysed in more detail by RNAi.

Hydroxyurea (HU) was recently used to synchronise procyclic form parasites. Here HU synchronisation is demonstrated in the human infective bloodstream stage, with 10 $\mu g.ml^{-1}$ shown to synchronise a population in S phase after 6 hours of exposure to the drug. Synchronised populations of *T. brucei* are then used to examine protein expression using western blots for the Rad51 paralogues Rad51-3 and Rad51-4, and to search for cell cycle regulated proteins more generally using Difference Gel Electrophoresis (DiGE). No cell cycle linked changes in protein levels were found using either method. RNAi-inducible cell lines were produced in both bloodstream and procyclic stages targeting the proteins ATM and ATR. Minor growth phenotypes were found for both proteins, post RNAi induction, in the procyclic stage, with 2 of 4 bloodstream stage *ATM* RNAi clones demonstrating a lethal phenotype and no growth phenotype being found in bloodstream stage *ATR* RNAi clones. Knockdown was demonstrated at the protein level in the *ATM* RNAi clones showing a lethal growth phenotype, but has not yet been shown in the remaining cell lines. The lethal phenotype appears to be linked to a failure to prevent DNA re-replication and segregate nuclei and kinetoplasts correctly.

Acknowledgements

This thesis is dedicated to Melinda, for her support and for holding onto my sanity until I needed it again.

Thanks are also due to the other members of the Hammarton and McCulloch labs for practical help and good times, as well as the other members of the 10.30 Tea Crew.

I would particularly like to thank Richard Burchmore and Alan Scott, without whom the DiGE and mass spectrometry would not have been possible, as well as my assessors, Jeremy Mottram and Harry de Koning for good advice and difficult questions.

Lastly, of course, my supervisors, Tansy Hammarton and Richard McCulloch, without whom this work would neither have started nor finished.

Declaration

I declare that this thesis and the results presented within are entirely my own work except where otherwise stated. No part of this thesis has been previously submitted for a degree at any other university.

Glynn Forsythe

Contents

List of figures

List of tables

List of Abbreviations: (in order of appearance)

ApoLI, apolipoprotein L-I; hpr, haptoglobin-related protein; hb, haemoglobin; TLF trypanosome lytic factor; SRA, serum resistance associated protein; BSF, bloodstream stage parasites; VSG, variable surface glycoproteins; DAPI, 4',6-diamidino-2-phenylindole; DSB, double stranded breaks; DDR, DNA damage response; PIKK, phosphatidyl inositol 3-kinase-like kinase; ATRIP, ATR Interacting Protein; HU, hydroxyurea; N, nucleus count; K, kinetoplast count; C, DNA content; DiGE, difference gel electrophoresis;

Introduction

Trypanosoma brucei is a single celled protozoan parasite spread by the tsetse fly (*Glossina* spp.) in sub-Saharan Africa. It causes Sleeping Sickness (more properly Human African Trypanosomiasis), an invariably fatal disease if untreated, and also infects cattle causing Nagana, an economically significant disease. After sustained effort, and during a drive to improve surveillance, reported cases have recently dropped below 10,000 per year, with an estimated 30,000 cases in total from 40,000 reported cases and an estimated 300,000 further in 1998 (WHO, 2010). There are three subspecies of *T. brucei*, distinguished by their ability to cause disease in humans: *T. brucei brucei* cannot infect humans due to lysis by apolipoprotein L-I (ApoLI) (Vanhamme *et al*., 2003), instead being a disease of cattle and wild animals; *T. brucei rhodesiense* causes an acute form of the disease; while *T. brucei gambiense* causes a chronic form and is responsible for an estimated 95% of human infections (WHO, 2010). ApoLI associates with haptoglobin-related (hpr) and haemoglobin (hb) proteins in the trypanosome lytic factor (TLF) complex, which is endocytosed after interaction with the parasites' hb-hpr receptor. ApoLI then forms pores when trafficked to the lysosome, leading to swelling of the lysosome and eventual cell death (Wheeler, 2010). Pore formation is inhibited in *T. b. rhodesiense* by SRA (Serum Resistance Associated) protein, while *T. b. gambiense* was recently shown to have downregulated expression of the hb-hpr receptor, with the *HpHbR* gene possessing polymorphisms causing a reduced affinity for TLF (Kieft *et al*., 2010; Wheeler, 2010).

T. brucei possesses a number of unusual features when compared with the more familiar "higher" eukaryotes, of which one good example is the single large mitochondrion possessed by these parasites. This mitochondrion changes structure based on the lifecycle stage of the parasite and contains genetic material stored in a cluster of interlinked rings known as the kinetoplast, from which many genes require post-transcriptional RNA editing to produce protein (Liu *et al*., 2005; Schneider *et al*., 2008; van Hellemond *et al*., 2005).

Lifecycle

As shown in Fig. 1, *T. brucei* infects a host after a bite from an infected tsetse fly releases metacyclic trypanosomes into the bloodstream. These then differentiate into slender bloodstream form trypanomastigotes, a proliferative stage that replicates by binary fission. On reaching high density within the mammalian host many of the slender form cells will differentiate into the non-proliferative stumpy form trypomastigote. If these are taken up by another tsetse bite they will infect the fly, becoming procyclic form cells, another

proliferative stage. After several more developmental changes the parasites migrate to the tsetse salivary glands, eventually becoming infective metacyclic cells (Vickerman, 1985) (Center for Disease Control, 2010). One of the factors that makes trypanosomiasis so deadly as a disease is the trypanosomes' ability to evade the host immune system by antigenic variation. The cell surface of bloodstream stage parasites (BSF) is coated by Variable Surface Glycoproteins (VSGs), which can be switched for any of thousands of alternatives within the *T. brucei* genome, which can themselves homologously recombine with each other or some of the many non-functional VSGs, producing an effectively unlimited library of possible antigens (Horn and McCulloch, 2010; McCulloch and Barry, 1999).

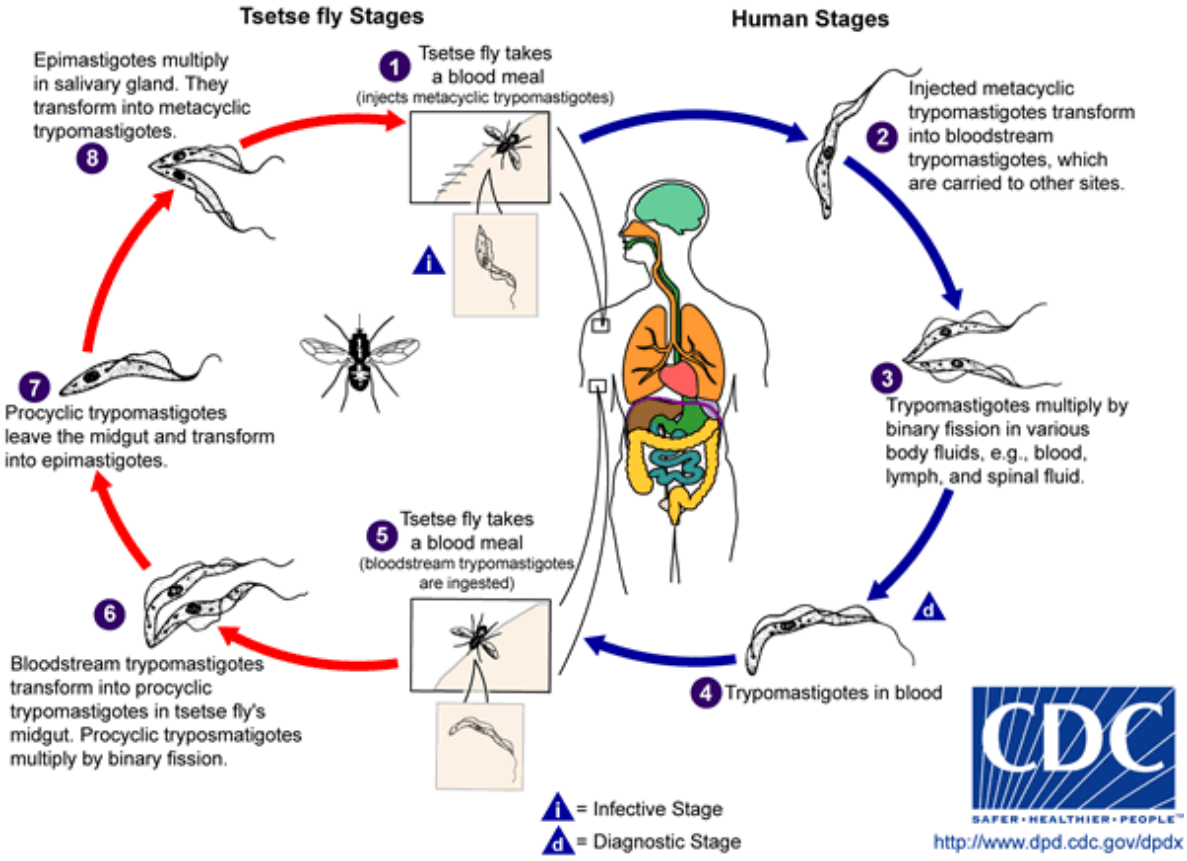

Figure 1 Lifecycle of *T. brucei* through the human infective and tsetse infective stages. (Center for Disease Control, 2010)

Cell cycle

The cell cycle of eukaryotic organisms is categorised as following G_0/G_1, S, G_2, M and cytokinesis stages. G_0/G_1 can be viewed as the base stage as this is where eukaryotes can pause mitotic replication. Rather than being an inactive stage, it is a period of cell growth as well as sensing of internal and external signals. Assuming those signals indicate that it is time to enter mitosis the cell will enter S phase, where DNA replication occurs. Following

this is another phase of growth, G_2, followed by segregation of the replicated DNA in M phase. Finally, the cell divides to form two daughter cells during cytokinesis (De Wulf *et al*., 2009). In *T. brucei* the nuclear and kinetoplast morphology of *T. brucei* can be examined by staining DNA with 4',6-diamidino-2-phenylindole (DAPI), together with cellular morphology, to provide a signpost to the cell cycle stage (Hammarton, 2007), as shown in Fig 2. Briefly, when there is a single nucleus and kinetoplast (a 1N1K configuration) the cell is in G_0/G_1. The kinetoplast S phase finishes slightly in advance of nuclear S phase, so it will divide ahead of the nucleus, giving a 1N2K configuration, which is indicative of nuclear S or G_2 phase (Woodward and Gull, 1990; Siegel *et al.*, 2008). During M phase the nucleus divides, giving a 2N2K configuration. Finally, cytokinesis begins from the flagellar tip and proceeds along the longitudinal axis, giving cells a distinct "two-tailed" appearance. Flow cytometry analysis after staining with propidium iodide also provides information on the proportion of cell populations in the various cell cycle stages, giving the proportion of cells with 2C DNA content (diploid cells), 4C (replicated DNA, G_2/M phase before separation into daughter cells) or an intermediate DNA content (S phase cells replicating DNA).

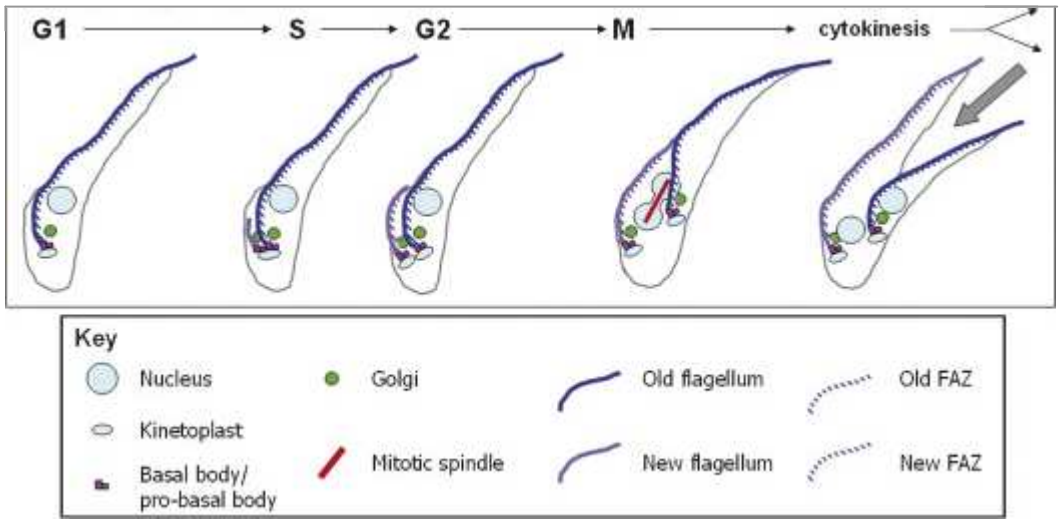

Figure 2: Cell cycle of *T. brucei* procyclic form parasites showing duplication and positioning of major single copy organelles. FAZ refers to the Flagellum Attachment Zone. (Hammarton, 2007)

The cell cycle can be paused at various stages, or checkpoints, to ensure that it progresses properly. The checks which must be passed include organelle segregation and proper chromosome attachment to the spindle (Glynn *et al*., 2010). The most interesting

checkpoints from the perspective of this introduction are those that occur after DNA damage to allow repair, as attempting to replicate damaged DNA may be impossible or lead to the introduction of errors (Shiloh, 2001). The process of detection of DNA damage and the cellular response to it will be discussed below, first generally and then specifically for *T. brucei*. Double stranded breaks (DSBs) in DNA can be repaired in several different ways depending on various factors including the cell cycle stage at which the break is detected. One of these, non-homologous end joining, has not been demonstrated in *T. brucei* (Burton *et al*., 2007), so will not be discussed. The main process of DSB repair in *T. brucei* is homologous recombination (HR), which is responsible for approximately 85% of DSB repairs (Glover *et al*., 2008) and is the focus of this project. The remainder of DSBs appear to be repaired by micro-homology mediated end joining, a process which is independent of many of the proteins essential for the other repair mechanisms (Burton *et al*., 2007; Glover *et al*., 2011).

DNA break detection and initial processing

There are two hypotheses describing DSB detection, although they are not necessarily mutually exclusive (Bekker-Jensen and Mailand, 2010). The first is that changes in chromatin structure after a DSB (which causes chromatin to relax for several megabases around the site of the break (Jaberaboansari *et al*., 1988)) activate the DNA damage response (DDR). Furthermore, other treatments, such as chloroquine (Krajewski, 1995) and exposure to hypotonic conditions (Earnshaw and Laemmli, 1983) also activate several proteins involved in the DDR and have been shown to alter chromatin structure (Bakkenist and Kastan, 2003). There is no known mechanism to translate this change in structure into protein signalling, although several necessary proteins have been found (Kanu and Behrens, 2008; Misri *et al*., 2008), of which the most important may be the acetylating protein Tip60 (Bekker-Jensen and Mailand, 2010; Sun *et al*., 2010).

More concrete and studied is the response initiated by the Mre11 complex (also known as the MRN or MRX complex) (Bekker-Jensen and Mailand, 2010). This complex consists of the proteins Mre11, Rad50 and one of the homologues Xrs2 or Nbs1 in yeast and vertebrate cells, respectively (Haber, 1998; Lee *et al*., 2007). Mre11 and Rad50 together are capable of binding DNA ends (for example at a DSB) and tethering them by interaction of the Rad50 “arms” of the complex either to other DNA ends or complete DNA strands (de Jager *et al*., 2001) and together with Nbs1/Xrs2 have been shown to be upstream of signalling molecules such as ATM (discussed below) in the DNA damage response. To complicate the picture, however, the Mre11 complex has also been shown to be involved in

many other aspects of the DNA damage response, and is also phosphorylated by some of the factors which it attracts and activates (D'Amours and Jackson, 2002). Immobilisation of the Mre11 or Nbs1 subunits on DNA has also been shown to be sufficient to activate ATM and the DDR (Soutoglou and Misteli, 2008).The Mre11 complex also has some 3' to 5' endonuclease activity, but together with several other proteins such as Exo1 and Sgs1 it is capable of the 5' to 3' resection necessary for processing DSBs (Rupnik *et al.*, 2010).

Signal transduction – the phosphatidyl inositol 3-kinase-like kinases

Many proteins are involved in the transmission of the DDR signals (Matsuoka *et al.*, 2007), but the main signalling molecules are the members of the phosphatidyl inositol 3-kinase-like kinase (PIKK) family. This family includes ATM, ATR, DNA-PK_{cs}, TOR, SMG-1 and TRAAP, all of which are stress response proteins. The PIKKs are an unusual family of kinases, as they possess a kinase domain related to a lipid kinase (phosphatidyl inositol 3-kinase), yet are mostly serine-threonine protein kinases (Abraham, 2004), with the exception of TRAAP, which appears to have lost its kinase function (Vassilev *et al.*, 1998). DNA-PK_{cs} is central to non-homologous end-joining DNA repair. The proteins relevant to homologous repair are ATM and ATR.

ATM

ATM stands for Ataxia-Telangiectasia Mutated protein. Ataxia-Telangiectasia is a disease in humans characterised by radiation susceptibility, neuronal degeneration, translocation between chromosomes, immunodeficiency and increased risk of cancer due to defects in repairing damaged DNA. It can be caused by many different mutations across the *ATM* gene (Chun and Gatti, 2004). In yeast the homologous protein is known as Tel1 (Harrison and Haber, 2006).

Inactive ATM exists in the nucleus as a dimer, with each ATM molecule blocking the other's kinase domain. On activation, whether by the Mre11 complex, or the unknown mechanism initiated by changes in chromatin conformation, the ATM molecules autophosphorylate and are released into a monomeric state. Each monomer is roughly 370 kDa in size (Bakkenist and Kastan, 2003) and activation is marked by phosphorylation at a serine residue in position 1981. Phosphorylation at this site appears essential for many processes, including monomerisation, interaction with downstream proteins and stabilisation of ATM at the DSB site (So *et al.*, 2009). Other proteins involved in the

activation of ATM include Protein Phosphatase 2A, which associates with ATM in undamaged cells to inhibit phosphorylation at serine 1981 and dissociates under genotoxic stress (Goodarzi *et al*., 2007), and Protein Phosphatase 5, which is necessary for full activation of ATM, with cells lacking functional protein phosphatase 5 having reduced ATM autophosphorylation (Ali *et al*., 2004).

ATR

ATR (ATM- and Rad3-related protein, occasionally referred to as Ataxia-Telangiectasia Related protein) has the homologues Mec1 and Rad3 in budding and fission yeasts, respectively (Harrison and Haber, 2006). It is slightly smaller than ATM, but is still a large protein, ranging from roughly 250 to over 300 kDa (Hall-Jackson *et al*., 1999).

ATR has both separate and overlapping functions with respect to ATM. It exists in a complex with ATRIP (ATR Interacting Protein), and activation occurs following the binding of this complex to Replication Protein A (RPA) (Shiloh, 2003). RPA rapidly coats any single-stranded (ss) DNA found in the cell, such as that produced by the Mre11 complex, stabilising the molecule and attracting ATR (Zou and Elledge, 2003), although the 9-1-1 complex is also required for activation (Ellison and Stillman, 2003). One of the main functions of ATR is the stabilisation of stalled replication forks, which are characterised by the presence of persistent ssDNA. However, ssDNA is also produced at the sites of DSBs by the action of the Mre11 complex. The original model suggested that this ssDNA/RPA complex directly recruited ATR into the DSB repair pathway (Shechter *et al*., 2004), but recent research suggests that the interactions are more complicated than this (Lee *et al*., 2007). Firstly, the Mre11 complex has been shown to bind to RPA (Olson *et al*., 2007). Although each has an independent DNA binding ability, and this has been mostly shown to be involved in checkpoint activation, it does not rule out some interaction between the factors during DSB repair. Secondly, the Mre11 complex has also been shown to associate with ATR and be a substrate of ATR (Lee *et al*., 2007).

Effectors

ATM and ATR are involved in the initiation of several different checkpoints: the G1/S phase checkpoint, through the phosphorylation of Cdc25A via p53, and the G2/M phase checkpoint through the phosphorylation of Cdc25C (Shiloh, 2001). There is also a transient S phase cell cycle arrest, mediated through Brca1 and SMC1 (Bakkenist and Kastan, 2003). This checkpoint is also activated in response to nucleotide depletion by

hydroxyurea (Grallert and Boye, 2008). These cell cycle checkpoints function to allow time for the DNA repair machinery to fix any damage before there are irreversible consequences, so we will first examine a few of the many mechanisms through which ATM and ATR initiate the checkpoints, then how homologous recombination repair of DSBs is effected through Rad51. The initial signal is mostly spread by the kinases Chk2 (or Rad53) for ATM and Chk1 for ATR. Although phosphorylated at the site of DNA damage, these proteins do not form foci, instead ranging throughout the nucleus and phosphorylating further proteins (Lukas *et al*., 2003).

The phosphatase Cdc25C is inactivated through phosphorylation on serine 216 by the kinases Chk1 and Chk2, mentioned above (Kiyokawa and Ray, 2008). This inhibits G2 to M phase cell cycle progression by preventing the activation of the cyclin-dependent kinase Cdc2. It also creates a binding site for the 14-3-3 protein, which exports and sequesters Cdc25C in the cytoplasm (Shiloh, 2001).S

In mammalian cells Brca1 is also integral to the DNA damage response. It is activated by phosphorylation by ATM, ATR and Chk2, with phosphorylation of serine 1387 engaging it in S phase checkpoint activation, while serine 1423 phosphorylation elicits G2/M phase checkpoint activation (Xu *et al*., 2001). Once activated, Brca1 has a range of activities, as it up-regulates p53 transcriptional activation (Ouchi *et al*., 1998), is essential for phosphorylation of Chk1 and activates transcription of several important proteins, such as 14-3-3 and Wee1 - an inhibitor of Cdc2 activity (Gudmundsdottir and Ashworth, 2006).

SMC1 (Structural Maintenance of Chromosomes) associates with Brca1 and is phosphorylated by ATM during the DSB response. SMC-1 proteins are also present in organisms which lack Brca1, being highly evolutionarily conserved. SMC1 is required for S-phase checkpoint activation (Yazdi *et al*., 2002). It has also been shown to be involved with homologous repair of DSBs (Schar *et al*., 2004), as have several other SMC proteins (Harvey *et al*., 2004), although the mechanism remains to be established.

The intra-S phase checkpoint is initiated by inhibition of CDC45 binding to late stage replication origins (Aparicio *et al*., 1999). However, it is unknown exactly how this is regulated, or even in many cases how late stage origins are distinguished from early origins (Grallert and Boye, 2008).

Repair proteins

HR repair of a DSB is performed by a group of proteins, of which Rad51 is a key member. Rad51 is a highly conserved protein, being homologous to bacterial RecA and archaeal RadA (Ogawa *et al*., 1993), which functions in a helical filament (Sung and Klein, 2006). It is activated by ATM via the tyrosine kinase c-Abl (Chen *et al*., 1999). This allows Rad51 to associate with Rad52 and the Rad51 paralogues, which displace RPA and load Rad51 onto the ssDNA produced at the DSB by the Mre11 complex and cofactors (Cahill *et al*., 2006).

The Rad51 paralogues are a group of proteins with some structural similarity to Rad51. The precise roles of the Rad51 paralogues are unclear, although some may function in the later steps of recombination (Sung and Klein, 2006). They are termed Rad55 and Rad57 in *Saccharomyces cerevisiae*, while humans possess the five proteins XRCC2, XRCC3 and Rad51B, -C and –D (Sung and Klein, 2006). Rad52 helps to load Rad51 onto RPA-coated DNA in yeast, although it may not be essential for this in mammals (San Filippo *et al*., 2008). The Rad51, aided by the Rad51 paralogues, and Rad52 then searches the genome for an unbroken homologous stretch of sequence, in an as yet undefined way (Barzel and Kupiec, 2008). Once it is found, Rad51 directs the invasion of the homologous region by the single stranded DNA, forming a “D-loop”. Polή (Pol eta) in humans, a Y family polymerase, then extends the invading strand in a Rad51-dependant process using the homologous DNA as a template (McIlwraith *et al*., 2005). The invading DNA may then be long enough to anneal to the 3’ overhang on the other side of the DSB (Smith *et al*., 2007). Alternatively, at some point during this process the second strand may also invade the homologous DNA, producing two Holliday junctions which cause crossover of DNA when resolved by Rad51 (Sugiyama *et al*., 2006).

Rad51 is sequestered by BRCA2 in every eukaryotic organism studied so far except some yeasts (Lo *et al*., 2003), which then delivers Rad51 to the site of damage (Agarwal *et al*., 2006). BRCA2 binds Rad51 with BRC repeats (Wong *et al*., 1997), which are present in varying numbers across different organisms (Lo *et al*., 2003).

Repair proteins in *T. brucei*

In *T. brucei* the core of the DSB sensing unit, Mre11 and Rad50 are present, though putative orthologues of Nbs1 or Xrs2 have not been identified. Mre11 knockout cell lines are still viable, but show reduced growth rates and an inhibited DNA damage response

(Robinson *et al*., 2002). The putative signalling molecules ATM and ATR have both been shown to be present by bioinformatic analysis (Parsons *et al*., 2005) and further elucidation of their role will be discussed in the results section.

The Rad51 homologous repair process has been studied in more detail in *T. brucei*. Rad51 itself is present and has been shown to be involved in homologous recombination (McCulloch and Barry, 1999). *T. brucei* also possess five Rad51 paralogues, termed DMC1 and Rad51-3, -4, -5 and -6. DMC1 does not appear to be involved (Proudfoot and McCulloch, 2006) in mitotic homologous recombination, but the others do (Dobson, 2009; Proudfoot and McCulloch, 2005) although possibly to varying extents. The presence of Rad52 has not been shown, however its functions may be covered by BRCA2 (Lo *et al*., 2003).

BRCA2 was identified in *T. brucei* some time ago (Lo *et al*., 2003). TbBRCA2 contains 15 BRC repeats, compared to 8 in humans and 1 to 4 in organisms more closely related to *T. brucei* (Hartley and McCulloch, 2008a; Lo *et al*., 2003). Hartley and McCulloch showed that this BRC repeat expansion is important for homologous repair in *T. brucei* although why it evolved is not clear.

Trypanosomes feature some unusual biology in their DDR. The first unusual response to DNA damage in *T. brucei* lies in cell cycle control. Research has shown that bloodstream form (BSF) cells appear to lack a checkpoint in response to the induction of DSBs via phleomycin, although other forms of DNA damage, such as alkylating agents, still induce a pause in the cell cycle, as do DSB-inducing agents applied to procyclic form parasites (R. McCulloch, personal correspondence, see Fig 3). The mechanical reason for this is currently unknown. Given the extremely wide ranging nature of their influence, however, we hypothesise that the ATM/ATR pathways and their coordination of the DNA damage response are involved. It is possible that BSF cells cannot afford to have a checkpoint for DSBs, as they are produced regularly in sub-telomeric regions (Boothroyd *et al*., 2009) during antigenic variation, which would continually interrupt the cell cycle. Glover *et al*.(2008) however, do see a build up of G_2/M phase cells after induction of a single DSB with ISceI, a disconnect with the previous evidence which may be caused by positional effects of the induced DSBs, or an inability of cells to continue replicating with broken DNA without initiating a true checkpoint.

A second unusual feature of the *T. brucei* response to DSBs is the lack of up-regulation of Rad51 expression in response to DNA damage, including phleomycin and MMS (R. McCulloch, personal correspondence), or loci-specific induction of a DSB via the controlled expression of the yeast ISceI meganuclease (Glover et al, 2008). Such up-regualation occurs in almost every organism studied across all three domains of life, including the closely related organisms *Trypanosoma cruzi* (Regis-Da-Silva *et al*., 2006) and *Leishmania major* (Mckean *et al*., 2001). Given the importance of homologous recombination in driving antigenic variation in *T. brucei* (McCulloch and Barry, 1999), we hypothesise that this has facilitated the evolution of constitutively high levels of Rad51 in the organism.

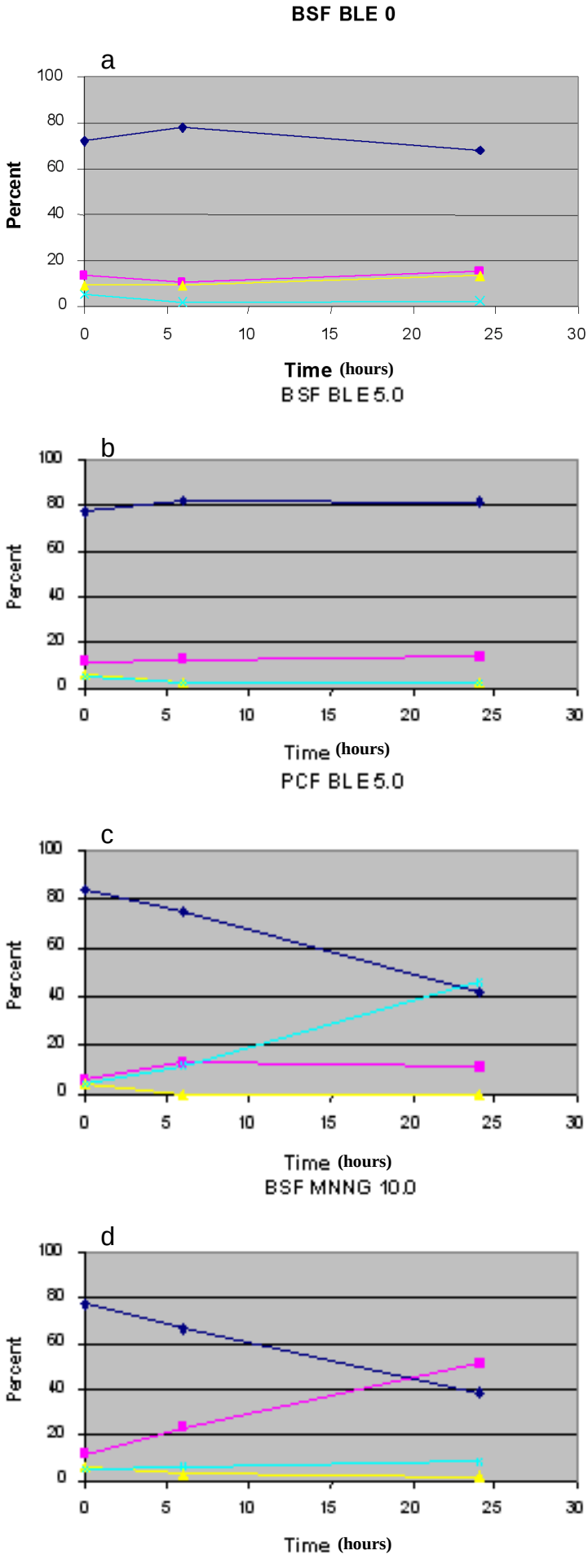

Figure 3: N-K configurations of *T. brucei* following DNA damage. Graphs show % of cells with variable ratios of DNA containing structures:
N = nucleus
K = kinetoplast
"Other" refers to abnormal configurations of N and K.

a: Profile of untreated 427 bloodstream form cells.

b: Profile of bloodstream form cells treated with 5µg.ml^{-1} of DSB-inducing agent phleomycin. Note little change in proportions of cell types. Total cell count decreases with time, however (data not shown).

c: Profile of procyclic form cells treated with 5µg/ml phleomycin. Decrease in 1N1K and 2N2K counts indicates cell cycle arrest.

d: Profile of bloodstream form cells treated with 10µg.ml^{-1} of the alkylating agent MNNG.

Figures by R. McCulloch, personal correspondence.

VSG Switching

As well as the survival of genomic insults, it has been shown that the DNA damage response is important for *T. brucei* in avoiding the host immune response. The *T. brucei* cell surface is covered in Variant Surface Glycoprotein (VSG, originally variant specific glycoprotein), a 400 – 500 amino acid protein with a highly variable N terminus (Carrington *et al*., 1991). These block access to less variable antigens on the cell surface and are periodically changed by the parasites in a process called antigenic variation, allowing a subpopulation to evade immune clearance and continue the infection (Marcello and Barry, 2007). Homologous recombination has been known to be involved in the process of antigenic variation for some time (McCulloch and Barry, 1999). More recently, induced DSBs were shown to produce VSG switching events, and native DSBs were demonstrated in sequence elements termed the 70 bp repeats proximal to *VSG* in the actively transcribed *VSG* expression site (Boothroyd *et al*., 2009), suggesting the importance of the DNA damage response to this process.

Aims and overview of results

This project examines the DNA damage response of *T. brucei* and its connection to the cell cycle through investigation of the core signalling molecules ATM and ATR and DNA damaging/checkpoint-inducing chemicals such as MMS and hydroxyurea.

A previously published method of synchronising the procyclic form (PCF) *T. brucei* (Chowdhury *et al*., 2008) with HU is adapted and validated for BSF cells. Initial attempts to use this to examine links between levels of DNA damage response proteins and the cell cycle stage do not detect any difference in *T. brucei* but leave room for further analysis. RNAi cell lines are produced for two DNA damage response signalling proteins ATM and ATR. BSF *ATM* RNAi gives a lethal phenotype in 2 out of 4 cell lines and knockdown levels are verified for those showing this phenotype. Knockdown is unable to be verified at this point for the PCF or BSF *ATR* cell lines, although the PCF cell lines both demonstrate a minor growth phenotype.

Methods

Chemicals:

Chemicals were sourced from Sigma unless otherwise stated.

Solutions were autoclaved at 15 psi, 121^{o}C for 20 minutes or filter sterilised as appropriate to ensure sterility.

Media:

Lurio Bertani (LB) broth used contains:

5 g NaCl,

10 g Tryptone,

5 g Yeast extract in 1 litre of distilled H_20.

LB agar used is as LB broth, plus 15 g agar per litre.

Bacterial media were supplemented with 100 μg.ml^{-1} ampicillin or 50 μg.ml^{-1} kanamycin where appropriate.

4 litres of HMI9 stock contains:

90.7 g of HMI9 powder (Invitrogen),

1.26 g $Na(CO_3)_2$,

71.5 μl β-mercaptoethanol,

H_2O to 4 litres.

For use 400mls of this is mixed with:

50 mls foetal bovine serum (GIBCO),

50 mls serum plus (JRH Biosciences),

50 units penicillin/streptomycin.

HMI9 was supplemented with 5 μgml^{-1} Hygromycin, 2.5 μgml^{-1} G418 and 2.5 μgml^{-1} Phleomycin where appropriate.

5 litres of SDM79 contains:

127.4 g of SDM79 powder (GIBCO),

1.26 g $Na(CO_3)_2$,

10 mls haemin,

H_2O to 5l,

Adjusted to pH 7.3 with NaOH.

For use, 450 mls of this is mixed with:

50 mls foetal bovine serum (GIBCO).

SDM79 was supplemented with 50 μg.ml^{-1} Hygromycin, 10 μg.ml^{-1} G418 and 10 μg.ml^{-1} Zeocin where appropriate.

Strains of *Trypanosoma brucei* used:

Wildtype Lister 427 strain *T. brucei brucei* BSF cells were used during hydroxyurea treatment. 427pLEW13pLEW90 BSF and 427pLEW13pLEW29 PCF strain *T. brucei brucei* (Wirtz *et al*., 1999) were used for transfection of RNAi vectors. Bloodstream form parasite cultures were grown in HMI9 at 37^{o}C with 5% CO_2 and kept below 1x10^6 cells.ml^{-1}, while procyclic form were cultured in SDM79 at 27^{o}C with 5% CO_2 between 1x10^6 and 1x10^7 cells.ml^{-1}.

Strains of *Escherichia coli* used:

Strataclone Solopack cells were used for cloning DNA fragments. Final vectors were transformed into XL1-Blue. Bacterial cultures were grown in LB broth at 37^{o}C with shaking at 200 rpm or on LB agar at 37^{o}C.

Minipreps and Maxipreps:

Qiagen QIAquick miniprep kits were used to extract plasmids from 5 mls of overnight *Escherichia coli* culture in LB broth in all cases except preparation of DNA for transfection, when a Sigma GenElute HP Plasmid maxiprep kit was used to extract plasmid from 100 mls of overnight culture. Kits were used as per manufacturer's instructions.

Gel electrophoresis:

0.8% w/v agarose in TBE gels were used. TBE is composed of:

5.4 gl^{-1} Tris,

2.75 gl^{-1} boric acid,

0.39 gl^{-1} EDTA in dH_20.

Gels were electrophoresed in TBE at 100 V using BioRad mini-sub or sub-cell gel tanks powered by BioRad power packs.

1kb+ ladder from Invitrogen was used as a marker.

TELT method of genomic DNA extraction:

100 mls of mid log phase PCF *T. brucei* were pelleted at 600 x *g* for 10 mins at room temperature. The pellet was resuspended in 100 mls of PBS, pelleted as before and resuspended in 5mls of TELT buffer

(2.5 M LiCl,
50 mM pH 8 Tris HCl,
62.5 mM pH 9 EDTA,
4% v/v Triton X-100)

then incubated at room temperature for 5 mins. This was then followed by phenol-chloroform extraction and isopropanol precipitation (see below). RNase A was added to 100 $\mu g.ml^{-1}$ and the reaction incubated at room temperature for 30 minutes. This was then removed by isopropanol precipitation as before.

Phenol-chloroform extraction:

1 volume of phenol was added and the suspension shaken by gentle inversion for 5 mins at room temperature. It was then centrifuged at 8978 x *g* at room temperature for 5 mins and the upper aqueous phase decanted. 1 volume of 24:1 chloroform:isoamyl alcohol was added and mixed and centrifuged as before. The aqueous phase was again decanted and the chloroform extraction repeated.

Isopropanol precipitation:

0.1 volume of 3 M pH 7 sodium oxaloacetate and 1 volume of isopropanol were added to the aqueous phase from above and vortexed. This was then centrifuged at 8978 x *g* for 15 mins at 4^oC. The pellet was resuspended in 1 ml of ice cold 70% ethanol and centrifuged at 8978 x g at 4^oC for 30 mins. The DNA pellet was air dried and resuspended in 500 µl of distilled H_2O.

Polymerase Chain Reactions:

Reaction volumes of 20 µl were used, containing:
2 µl of the relevant reaction buffer (to a final concentration of 1x),

2.5 mM of dNTPs,

25 mM Mg^{2+}

10 ng.μl^{-1} of each primer (listed in Table 2.1),

1 unit of polymerase enzyme (either Taq or Pfu Turbo from New England Biolabs),

200-500 ng of DNA (colony PCRs had small amounts of the respective colony added by sterilised toothpick).

Taq PCR was performed under the following program:

1 x 95^{o}C for 30 secs (5 minutes for colony PCR)

30 x 95^{o}C for 50 secs, 50^{o}C for 50 secs, 70^{o}C for 1 min

1 x 72^{o}C for 5 mins

Pfu Turbo PCR was performed under the following program:

1 x 95^{o}C for 30 secs

30 x 95^{o}C for 50 secs, 50^{o}C for 50 secs, 70^{o}C for 3 mins

1 x 72^{o}C for 5 mins

After Pfu Turbo use A-tailing was performed at 72^{o}C for 10 mins with Taq polymerase using:

19.5 µl of Pfu Turbo reaction,

5 µl of 10x buffer (inc. $MgCl_2$ and dNTPs)

0.5 µl Taq

Table 1: Primers used in PCR reactions (restriction sites underlined and named in brackets).

Name	Gene	Sequence 5’ – 3’
OL2078	*GFP* sense	GGCGGGATCCACTTGACGTGAGCAAGGGCGAG (*Bam*HI)
OL2708	*mCherry* sense	GAAAGGATCCATGTACCCCTACGACGTCCCGGACTATGCCGCAACTAGCGGCATGGTTAG (*Bam*HI)
OL2084	*GFP* antisense	CTTTCTCGAGCTTGTACAGCTCGTCCATGCC (*Xho*I)
OL2755	*ATM* 5’ UTR	GAATCCGCGGGGTGAATAGAGTTGGGG (*Sac*II)
OL2756	*ATM* 5’ UTR	GGAGTCTAGAAATCACGGATTCGATGTTTG (*Xba*I)
OL2757	*ATM* ORF	CCACCTCGAGTCAGCCTCACAAGATGCC (*Xho*I)
OL2758	*ATM* ORF	GGAGGGTACCGGAAGAGGAAGAGGAATGGG (*Apa*I)
OL2759	*ATR* 5’ UTR	GGTTGATATCGCGTATGCACAGCCTCTGC (*Eco*RV)
OL2760	*ATR* 5’ UTR	GGTAGAATTCCCACTTGCAGCTGAAAATCG (*Eco*RI)
OL2761	*ATR* ORF	GAAGCCGCGGGAGATAGATGCGGAAAACG (*Sac*II)
OL2762	*ATR* ORF	GAAACCGCGGCAGCTGCAGTAGAAGCGGC (*Sac*II)
OL2763	*ATM* RNAi fragment	GAAAGGATCCCGGATGACATGGAATGCG (*Bam*HI)
OL2764	*ATR* RNAi fragment	CCTTCTCGAGCCGATGACCTCCTCCTGG (*Xho*I)
PR29	*mCherry* antisense	GGAGTCTAGATGCGGTACCAGAACCTTTG (*Xho*I)
PR67	*ATR* 5’ UTR -> *NeoR* antisense	GTAAATAACTGTAAGGAAGTTGCCCAAAGCGTTATAGGCTGTTTTGCATTCGATTTTCAGCTG

		CAAGTGGATGATTGAACAAGATGGATTG
PR68	*ATR* ORF -> *mCherry* sense	AAAATCGATTATGTTCGGTCACGTTACCCGG CGATGTGACAATGGTAACAACGTTTTCCGCA TCTATCTCTGCGGTACCAGAACCTTTG
PR69	*ATM* 5' UTR -> *BlastR* antisense	AAACGAAAAGCGGATACACATAAACACGAG AGGGTATAAGTTGTAGTCATCAAACATCGAA TCCGTGAATTATGGCCAAGCCTTTGTCTCAG
PR70	*ATM* ORF -> *GFP* sense	TACTCCGCTGCGACACTGCCGGATGCCGTCC CCTAAACAATCCAAGCATTGAGGCATCTTGT GAGGCTGACTTGTACAGCTCGTCCATGC
PR81	*ATR* for RT-PCR sense	GTGCAACGTTGGCTGTATGG
PR82	*ATR* for RT-PCR antisense	TCTAGTATCGCCGGCAGCTT
PR83	*ATM* for RT-PCR antisense	CCAAATGCTGGTCTGGTAATCA
PR84	*ATM* for RT-PCR sense	CCCCATGCGTCGAATTGA
PR85	*CDC14* for RT-PCR sense	GGTGTCGTGCGTCTTAACGA
PR86	*CDC14* for RT-PCR antisense	TGAATACCGCGCGAAAGAA
PR160	*ATR*-*Sac*II sense for RNAi fragment	CCGCGGCGCTCCCTTAAGTGCAAAAG (*Sac*II)
PR161	*Xho*I-*ATR* antisense for RNAi fragment	CTCGAGCGAATTCCCTCCAATGAAGA (*Xho*I)
PR214	VSG 221 sense	AGCTAGACGACCAACCGAAGG
PR215	VSG 221 antisense	CGCTGGTGCCGCTCTCCTTTG
PR216	VSG VO2 sense	GTAAACGGTCCGGAGTTCAA
PR217	VSG VO2 antisense	CATTTCCGCGTTGTCTTGTA
PR218	VSG 121 sense	ACCTGACATCGGACGGTAAC
PR219	VSG 121 antisense	GTCGGTTATGTCGGCAAGTT
PR220	VSG 224 sense	AGGAAATAGCGTCGCTCAGA
PR221	VSG 224 antisense	TTCTTTTCCATCCCATTTGC
PR222	BC118 sense	CAGAAGCGCCAATACAACAA

PR223	BC118 antisense	CGTTAGAAACCACGCCAGTT
PR224	BC222 sense	CGGAAGAGACAATTCGAAGG
PR225	BC222 antisense	CGCCATTGACATCCCTACTT
PR238	*ATM* RT-PCR fragment antisense	GGATAAACCGCGCGTAGATG
PR239	*ATM* RT-PCR fragment sense	CGGCGAGTCACTCCTTGGT
PR275	*Xho*I-*ATR ORF* sense	CTCGAGGAGATAGATGCGGAAAACGTTGTTA (*Xho*I)
PR276	*Not*I-*ATR ORF* antisense	GCGGCCGCAAAATGCAGTGAATGAGGATAG CCG (*Not*I)
PR277	*Not*I-*ATR 5'UTR* sense	GCGGCCGCTATGCACAGCCTCTGCGCTATAC AT (*Not*I)
PR278	*Bam*HI-*ATR 5'UTR* antisense	GGATCCCCACTTGCAGCTGAAAATCGAATGC (*Bam*HI)
PR279	*attB4-Not*I-*ATM 5'UTR* sense	GGGGACAGCTTTCTTGTACAAAGTGGGCGGC CGCCGCTCGTGTGAAGGAGAAACGGCTC (*Not*I)
PR280	*attB1R-ATM 5'UTR* antisense	GGGGACTGCTTTTTTGTACAAACTTGAATCAC GGATTCGATGTTTGATGAC
PR281	*attB2r-ATM 3'UTR sense*	GGGGACAGCTTTCTTGTACAAAGTGGGCGTC CATTACGCGTTTGGTTGTTC
PR282	*attB3-Not*I-*ATM 3'UTR* antisense	GGGGACAACTTTGTATAATAAAGTTGGCGGC CGCGGGTAGTAGGAGGATGCATTACTTA (*Not*I)
PR283	*attB4*-NotI-*ATR 5'UTR* sense	GGGGACAGCTTTCTTGTACAAAGTGGGCGGC CGCACCCTTTTTGCGTATGCACAGCCTC (*Not*I)
PR284	*attB1r-ATR 5'UTR* antisense	GGGGACTGCTTTTTTGTACAAACTTGCCACTT GCAGCTGAAAATCGAATGC
PR285	*attB2r-ATR 3'UTR* sense	GGGGACAGCTTTCTTGTACAAAGTGGTGATG TGCTGCCACCACTGCGGAT
PR286	*attB3-Not*I-*ATR 3'UTR* antisense	GGGGACAACTTTGTATAATAAAGTTGGCGGC CGCTTGCCTCCCCACTTGTAAAGATGAG (*Not*I)
PR287	*ATM antisense for*	CAGTTACCTCGGCTC

	northern blot probe with PR239	
PR300	*ATR* probe for Northern blot	CAATAACGTCTACACTTC
β tub f	β tubulin sense	GCCCCGACAACTTCATCTTTGGA
β tub r	β tubulin antisense	TTTCGCATCGAACATCTGCTGCG

Table 2: Plasmids used

Name	Description	Reference
p2T7/GFP	RNAi vector with opposing T7 promoters	LaCount *et al.* 2000
pSC-A	Cloning vector	Stratagene
pSC-B	Cloning vector	Stratagene
pHG13	*ATM* RNAi	This study
pHG104	mCherry:*ATR* endogenous tagging construct	This study
pHG105	eGFP:*ATm* endogenous tagging construct	This study
pHG146	*ATR* RNAi	This study

Cloning:

A-tailed gene fragments produced by PCR were cloned into the pSC-A cloning vector from Stratagene according to the Strataclone Solopack PCR cloning kit instructions. Blunt ended fragments were cloned into pSC-B using the Strataclone Blunt-Ended Cloning Kit. Presence and orientation of gene fragments were confirmed by restriction digests and the plasmids sequenced by The Sequencing Service (Dundee). These fragments were then digested from the cloning vector and ligated into a final vector which had been digested by the same enzyme(s).

Ligation:

Ligation was by T4 DNA ligase using a 3:1 insert:vector molar ratio with 1 μl (400 units) of DNA ligase in 10 μl at 4^{o}C overnight.

Transformation into XL1-blue:

5 μl of ligation reaction was added to 50 μl of competent *E. coli* XL1-Blue cells and the mixture incubated on ice for 30 mins. They were then given a 45 second heat shock at 42^{o}C and returned to ice for 2 mins. 1 ml of 37^{o}C pre-warmed LB broth was added and they were incubated at 37^{o}C for 1 hour. The cells were pelleted using a benchtop centrifuge at 13000 rpm for 5 mins, 900 μl of supernatant were removed and the cells resuspended in the remainder. 5 and 10 μls were then plated onto ampicillin containing LB agar plates. Colonies picked from these plates were tested for plasmid presence by colony PCR and digesting minipreps from overnight cultures.

Preparation of DNA for transfection:

Plasmids from maxipreps of overnight cultures were linearised by overnight NotI digestion and purified by phenol-chloroform precipitation as for genomic DNA.

Transfections

Cell lines were transfected with 10 μg DNA per 3 x 10^{7} cells using the Amaxa nucleofector program X-001. They were then left to recover in media without drugs (HMI-9 for BSF trypanosomes and SDM-79 for PCF cells) for a minimum of 6 hours before selective drugs were added. PCF transfections used 30% conditioned medium.

Conditioned medium was produced by growing PCF cells in SDM79 past $1x10^7$ cells.ml^{-1} for 3 days then mixing this with fresh SDM79 in a 1:1 ratio.

Counting *T. brucei* cell density:

Cell density was measured with an Improved Neubauer counting slide (Hawksley).

Calculating generation time for log growth phase cells:

The formula used was:

$k = (N_t-N_0)/(t \times \log 2)$

Where: k = number of generations per unit time

N_t = number of cells at time t

N_0 = number of cells at time 0

The generation time is then 1/k.

Removal of cells from hydroxyurea-containing medium:

Cells were pelleted at 1500 x *g* for 10 mins, washed with drug-free HMI-9 twice (with centrifugation repeated) and finally were resuspended in HMI-9 without hydroxyurea.

4',6-diamidino-2-phenylindole (DAPI) staining

5×10^5 cells were dried onto microscope slides and fixed with -20^{o}C methanol for > 1 hour. The cells were rehydrated with PBS for 5 minutes, than a drop of VectaShield DAPI and mounting medium (Vector Laboratories Inc.) added. A cover slip was placed over the top and sealed with nail varnish. Slides were examined using an Axioskop 2 microscope and Openlab 4.0 software. 200 cells were counted at each time point.

Immunofluorescence

Immunofluorescence was performed as described in Ambit (2006). Briefly, 5×10^5 cells were washed in trypanosome dilution buffer (TDB: 20 mM Na2HPO4, 2 mM NaH2PO4, 80 mM NaCl, 5 mM KCl, 1 mM MgSO4, 20 mM glucose, pH 7.4) and fixed in 1% formaldehyde. They were then permeabilised by the addition of 0.1% Triton X-100 and incubated for 10 minutes at room temperature. 1 M Glycine in phosphate buffered saline (PBS) was then added to a final concentration of 0.1 M and the cells were

incubated for 10 mins at room temperature before being settled onto poly-l-lysine coated slides. 20 µl of KMX antibody (Birkett *et al*., 1985) were added and the slides incubated overnight at 4 ^{o}C in a humid chamber. The slides were then washed with PBS and incubated with a 1/1000 dilution of Alexa Fluor 488-conjugated anti-mouse IgG secondary antibody in PBS for 1 hour in the dark. After another PBS wash, VectaShield DAPI and mounting medium was added and a coverslip applied. Fluorescence was observed using a DeltaVision RT microscope system (Applied Precision) and image stacks in the z plane were captured with a Roper CoolSnap-HQ 12-bit CCD camera controlled by SoftWoRx software and deconvolved. Twenty cells were examined for each cell type at each time point measured.

Flow cytometry

10^6 cells per sample were fixed in 70% methanol 30% PBS at 4^{o}C overnight. They were then washed in PBS and resuspended in PBS containing 10 µg.ml^{-1} propidium iodide and RNase A. This was incubated for 45 mins at 37^{o}C in the dark, then analysed using a FACScalibur machine.

Western Blotting

10^5 cells µl^{-1} were resuspended in 1x NuPAGE loading buffer (Invitrogen, as per manufacturer's instructions) and heated to 70^{o}C for 10 minutes. 10 µl (10^6 cells) were loaded per lane on 3-8% Tris Acetate (TA) or 20% Bis-Tris gels (Invitrogen) and electrophoresed with TA or MOPS buffer respectively as per manufacturer's instructions. Protein was then transferred onto nitrocellulose membrane (GE Healthcare) and blocked overnight in PBST+M (PBS containing 0.1% Tween and 5% w/v milk powder) at 4^{o}C.

Antibodies diluted in PBST+M were incubated with the membrane for 1 hour at room temperature. The membrane was washed three times in PBST for 15 minutes each, then incubated with the secondary antibody (conjugated to HRP) in PBST+M for an hour and the washing steps repeated. The membrane was incubated with developing solution from the West Dura or West Femto kit (Pierce) and imaged using Kodak film.

Table 3: Antibodies used in western blots

Primary Antibody	Dilution	Secondary Antibody	Dilution
Rad51-3	1:10	Goat anti-rabbit	1:5000
Rad51-4	1:100	Donkey anti-sheep	1:5000
polyclonal anti-GFP (ab6556)	1:1000	Goat anti-rabbit	1:5000
OPB	1:1000	Donkey anti-sheep	1:5000

RNA extraction and electrophoresis

10^8 cells were harvested by centrifuging at 1500 x *g* for 10 mins (BSF) or 600 x *g* for 10 mins (PCF). Induced samples were with 10 μg.ml^{-1} tetracycline for 18 hours prior to harvesting. RNA was then extracted using the Qiagen RNeasy kit on a Qiacube automated system with on-column DNase digest according to the manufacturer's instructions. 5 μg of each RNA sample were re-digested with Ambion RNase free DNase I at 37^{o}C for 1 hour. 1 μg of each sample was then separated by electrophoresis on a 1.5% agarose gel containing 2.2 M formaldehyde and transferred onto nylon membrane by capillary transfer overnight in 20x SSC buffer (3 M NaCl, 300 mM sodium citrate, pH 7).

Northern blotting

Probes for northern blotting were contructed using the PrimeITII kit (Stratagene) according to manufacturer's instructions with primer pairs PR287 and PR237 (*ATM*), PR300 and PR81 (*ATR*) and β tubulin forward and reverse primers (see Table 2.1).

Hybridisation was performed at 50^{o}C overnight in 0.5 M Church Gilbert solution (342 mM Na_2HPO_4, 158 mM NaH_2PO_4, 7% w/v SDS, 1 mM EDTA) and the blots were exposed against storage phosphor screens (GE Healthcare) for 4+ hours and scanned on a Typhoon 8610 Variable Mode Imager.

DiGE Sample Collection

Between 1x10^8 and 1x10^9 of either untreated or HU synchronised wt 427 PCF cells were harvested by centrifugation at 600 x *g* and washed twice in ice cold PBS, removing as much supernatant as possible with a pipette after the second wash. Cells were resuspended in ice cold lysis buffer (7M urea, 2M thiourea, 4% CHAPS and 30 mM Tris–base, pH 8.0) with 100 μg.ml^{-1} DNaseI (Invitrogen), 5 mM $MgCl_2$ and 1 x final concentration of

Complete EDTA free inhibitor cocktail (Roche), at a concentration of 10^9 cells.ml^{-1}. Cells immediately lysed using 3 x 1 second cycles of probe sonication (MSE Soniprep) with 1 minute of cooling on ice between sonications. After a 10 minute incubation at room temperature the mixture was centrifuged at 13000 x *g* for 10 minutes and the supernatant transferred to a fresh microcentrifuge tube. 4 x sample volume of -20^{o}C acetone was added and the tube vortexed and incubated at -20^{o}C for >1 hour. Centrifugation was repeated and the pellet washed with 4 volumes of -20^{o}C 80% acetone, 20% lysis buffer, then the pellet was air dried for roughly 5 minutes. The pellet was resuspended in 200 µl of lysis buffer + protease inhibitors, centrifugation was repeated and the supernatant transferred to a fresh tube, the protein content was adjusted to a final concentration of 5 µg.ml^{-1}.

CyDye Labelling

CyDye labelling was performed as described in the CyDye DiGE Fluor labelling kit (Amersham biosciences). Briefly, 50 µg of protein sample was mixed with 4 nM of CyDye and incubated on ice in the dark for 30 minutes. Lysine was added to 1 mM to stop reaction, and the mixture incubated a further 10 min on ice in dark. HU synchronised and untreated samples were paired, with one of each labelled with Cy3 and the other with Cy5, these were then mixed together before loading onto gel. The CyDye used for each sample was alternated to account for any preferential labelling.

DiGE

1st Dimension separation was by isoelectric point using 24 cm immobilised pH gradient (IPG) strips (pH 4 – 7) on an Ettan Dalt IPGphor system (GE Healthcare) overnight at 8 W (2 W per gel). The IPG strips were then laid on top of 12% acrylamide gels and sealed with a 0.5% (w/v) agarose solution. Gels were electrophoresed at 50 V for 18 hours and the gels were scanned using a Typhoon 9400 scanner (GE Healthcare). Cy3 was scanned at 532/580 nm and Cy5 at 633/670 nm excitation/emission wavelengths respectively. Images were cropped using Imagequant software and analysed with DeCyder 5.1 software (GE Healthcare).

Mass Spectrometry

Spots were picked by hand and digested with 0.2 µg.µl^{-1} modified Porcine Trypsin (Promega) in 25mM ammonium bicarbonate overnight at 37^{o}C and analysed by electrospray ionization mass spectrometry on a Q-STAR® XL Hybrid LC/MS/MS System.

Results were analysed with Analyst QS 1.1 software (Applied Biosystems) and the automated Matrix Science Mascot Daemon server (v2.1.06).

Results 1

Hydroxyurea synchronisation

Cell cycle synchronisation is a useful tool in many other organisms (Lee *et al*., 2011; Schorl and Sedivy, 2007; Valero *et al*., 2011), and potentially especially useful for this project given the link between cell cycle control and the DNA damage response (Cook, 2009; Derheimer and Kastan, 2010; Lopez-Contreras and Fernandez-Capetillo, 2010). In addition hydroxyurea (HU) has previously been shown to activate ATR in other organisms (Ward and Chen, 2001), which suggested that it may be directly useful as a tool for further study in this project. Although unsuccessful attempts at HU synchronisation of *T. brucei* BSF had been made in the past (Mutomba and Wang, 1996), fortuitously, HU synchronisation of the procyclic form (PCF) had recently been demonstrated (Chowdhury *et al*., 2008). This chapter will focus on adapting the techniques shown in this more recent publication to synchronise the bloodstream stage (BSF) parasites.

Hydroxyurea is hypothesised to produce a stall in the cell cycle by inhibition of nucleotide reductase. This prevents the production of dNTPs, preventing formation of new DNA once the cellular pool of dNTPs is exhausted. This eventually initiates an S phase checkpoint (Allen *et al.* 1994; Grallert and Boye, 2008). A delay between hydroxyurea application and the depletion of the cellular dNTP pool explains some of the phenomena shown below, further the inhibition of nucleotide reductase appears to be incomplete as cells progress slowly through S phase in both other organisms and *T. brucei* (Allen *et al.* 1994; Chowdhury *et al.* 2008 and see below).

To attempt to identify a dose of HU that may be appropriate for cell cycle synchronisation, BSF *T. brucei* parasites were incubated with a range of HU concentrations and their growth analysed (Fig. 4). It was hypothesised that a useful HU concentration would lead to a decrease in growth rate, potentially indicating cell cycle stalling, without immediately killing the parasites, which may indicate irreversible cell death. A concentration of 5 $\mu g.ml^{-1}$ HU had only a minor effect on growth rate. The effect was more pronounced with 7.5 $\mu g\ ml^{-1}$ HU, but the parasites continued to replicate until 18 hours after addition of the drug. Concentrations from 10 $\mu g.ml^{-1}$ HU upwards arrested growth after around 9 hours, with longer exposure being lethal, therefore 10 $\mu g.ml^{-1}$ was examined more closely, as it was the least concentrated level to rapidly inhibit population growth.

Having found an appropriate concentration to examine, the next step was to determine whether cell cycle synchronisation was occurring and, if so, what duration of treatment might be appropriate. To this end BSF cells were exposed to 10 μg ml^{-1} HU and samples taken for flow cytometry analysis and DAPI staining every 2 hours. The flow cytometry profile (Fig. 5) before addition of HU (t = 0) shows a typical asynchronous population of cells, with large peaks in DNA content at 2C (G_1 phase) and 4C (cells with fully replicated DNA, ie. G_2, M or cytokinesis phases) and some cells in between with an intermediate DNA content (S phase cells). After just 2 hours, the population had formed a peak of 2C DNA content with a slight tail running through 4C. The position of the peak progressed to the right, being roughly central between 2C and 4C at 6 hours of incubation and largely at 4C after 10 hours.

This fits well with the data from N and K counting after DAPI staining (Fig. 6). There, the amount of 1N1K (i.e. G_1 and early S phase) cells increased from 70 to 80% at 2 hours, followed by a decrease in 1N1K and increase in 1N2K (S phase/G_2) cells until 8 hours. 2N2K (M and later phases) cells were not visible by 4 hours as they progressed through cytokinesis to the beginning of the cell cycle, with a small amount (<5%) appearing at 8 hours and increasing to 10% by 10 hours. This suggests that some cells escaped the S phase block and progressed completely through the cell cycle.

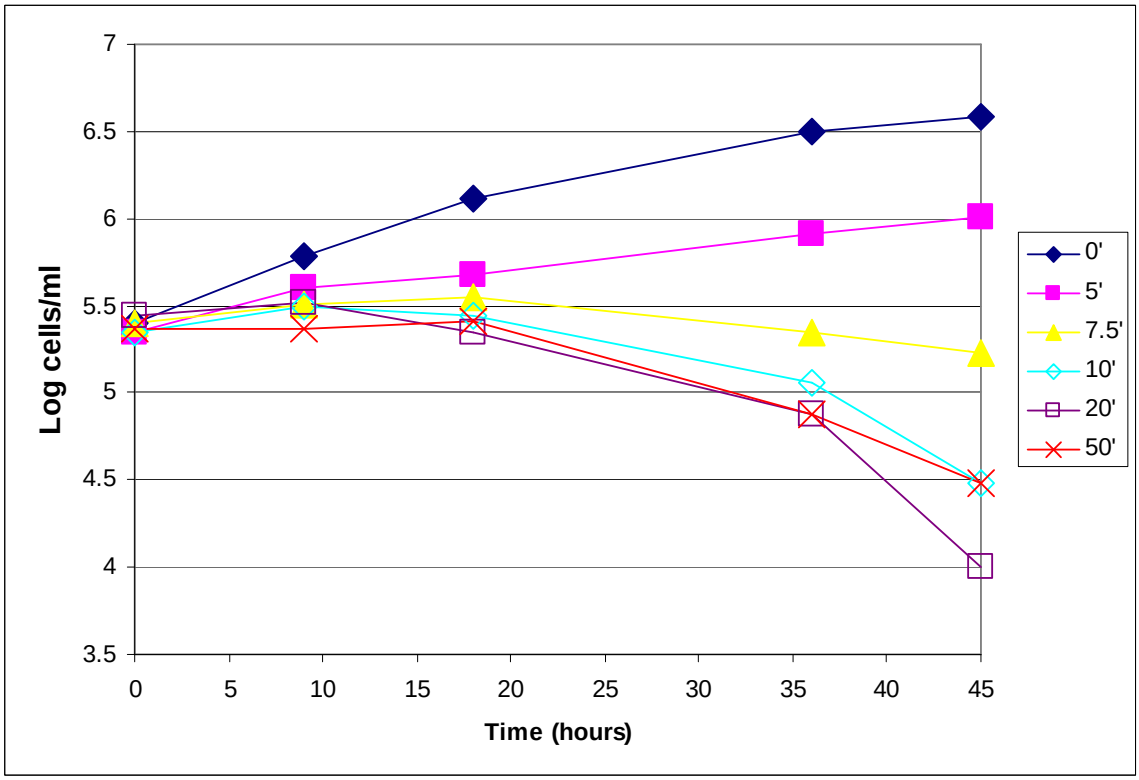

Figure 4: Cumulative growth curve of BSF cells incubated with 0 (♦), 5 (■), 7.5 (▲), 10 (◊), 20 (□) or 50 (x) $\mu g.ml^{-1}$ HU.

These results suggested 6 hours to be the optimum incubation time to substantially enrich for a population of cells in S phase, and so cells under these conditions were analysed further. 1N1K cells are potentially a mix of cells in G1 and S phases. Since the kinetoplast S phase is slightly in advance of, and finishes sooner than, nuclear S phase, kinetoplast morphology can be used to determine the proportion of 1N1K cells in G_1 or S phase. Kinetoplasts elongate in S phase, then form v and finally bone shapes before separating into two distinct kinetoplasts. These stages are shown in the insets of Fig. 7.

The hypothesis was that cell populations treated with HU should have a higher proportion of 1N1K cells in S phase, as measured by kinetoplast length. The kinetoplast length was measured using Openlab 4 software after DAPI staining. As observed elsewhere (Hammarton *et al*., 2007) kinetoplast length showed several peaks (Fig. 7). The first (~0.3 – 0.89 μm) represents round or oval kinetoplasts either yet to begin replication or very early in S phase, the second (~0.93 – 1.19 μm) comprises v shaped kinetoplasts and the third (>1.2 μm) comprises bone shaped kinetoplasts. The untreated population showed a majority of 1N1K cells with small kinetoplasts, while the majority (72/102) of HU treated 1N1K cells showed the long morphologies indicating replication. This is likely to be an underestimate, as some of the smaller kinetoplasts are almost certain to be merely too early in S phase to have extended measurably, but the high proportion here together with the data from DAPI counts indicates that at least 90% of cells treated with HU for 6 hours are in S phase. This is a significant enrichment over untreated populations.

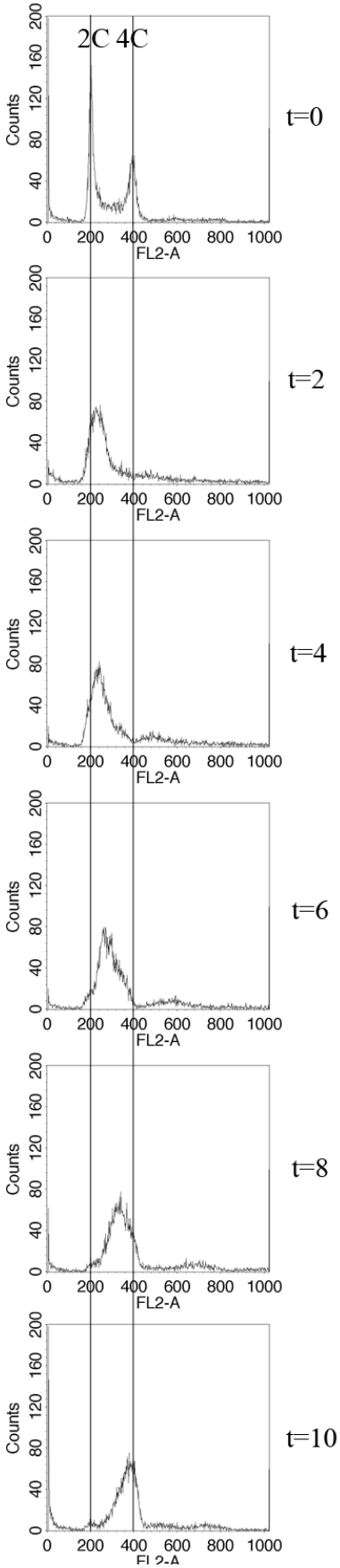

Figure 5: Flow cytometry profiles of DNA content in cells incubated constantly with 10 μg.ml^{-1} HU for t hours. Vertical lines show position of 2C and 4C DNA content.

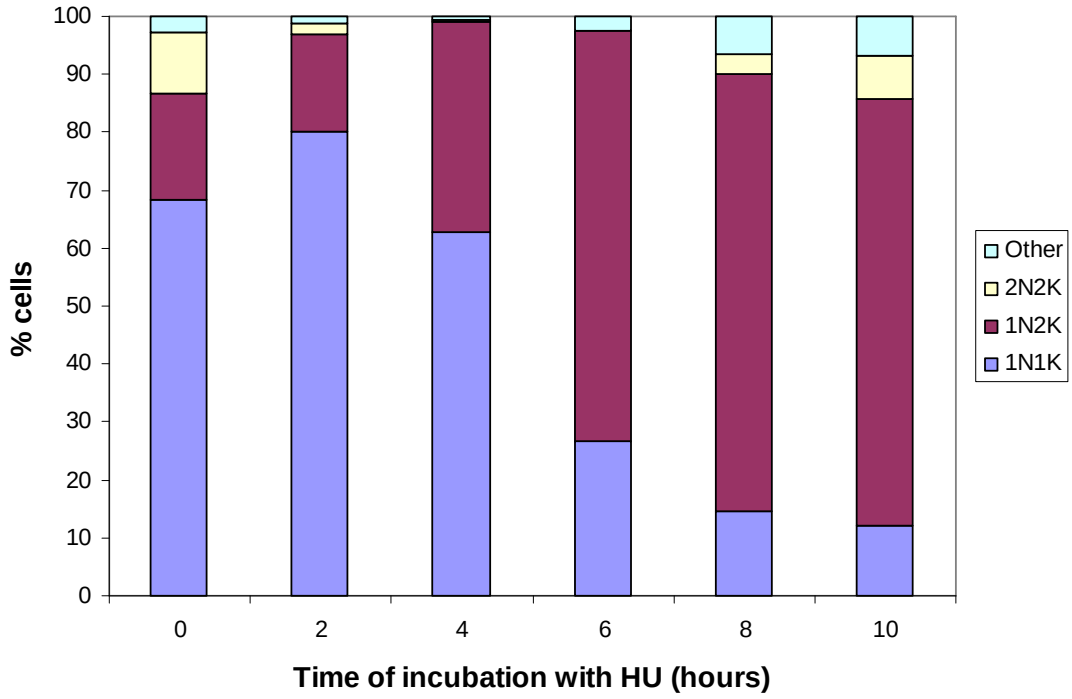

Figure 6

Nucleus (N) and kinetoplast (K) counts of cells sampled at the same time points as in Figure 5, as shown by DAPI staining. "Other" represents abnormal configurations. n>200 for each time point.

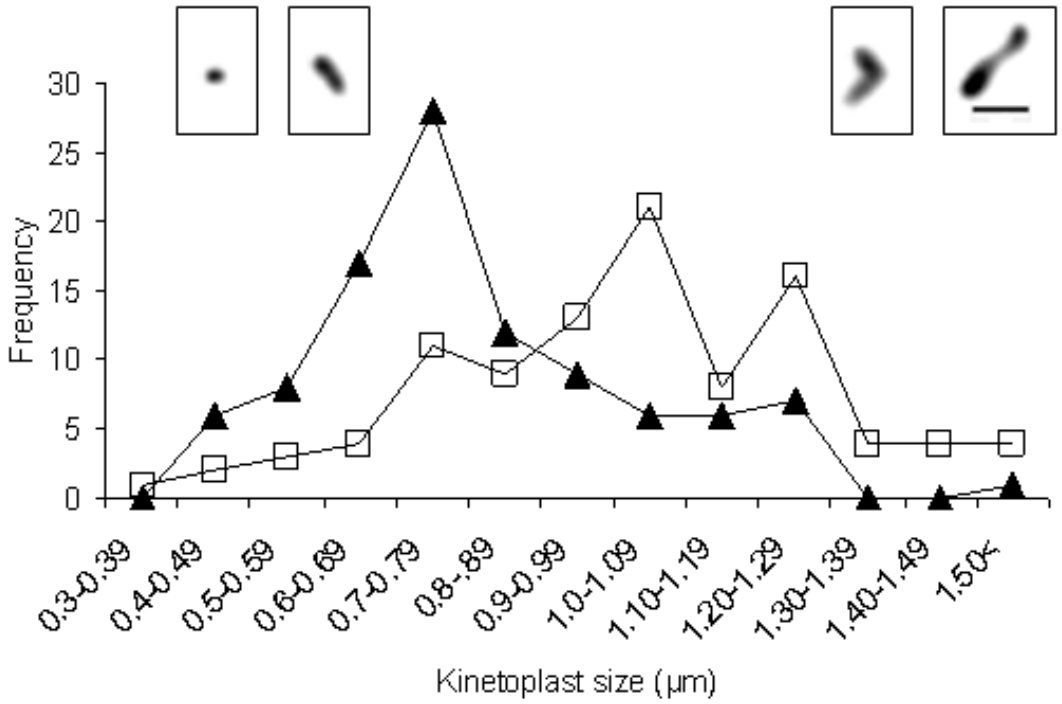

Figure 7

Kinetoplast size from 1N1K cells before (▲) and after (□) 6 hours incubation with 10 µg ml^{-1} HU. Insets show examples (running left to right) of round, oval, v shaped and bone shaped kinetoplasts from 1N1K cells. Scale bar in right inset shows 1 µm. n=100.

HU synchronisation would be a more powerful tool if able to give populations enriched for phases other than S. Also, it would be less useful as a tool if the S phase population was overly damaged by the treatment. To assess these issues populations of cells were treated with HU for 6 hours then washed and resuspended in fresh media to remove the HU. Growth curves (Fig. 8Figure 8) showed that growth returned to pre-treatment rates within 6 hours. Cell cycle progression after S phase was monitored by flow cytometry and DAPI staining (Fig. 9 and Fig. 10). For the first 2 hours after release the S phase flow cytometry peak (Fig. 9) progressed towards 4C, while the DAPI count (Fig. 10) remained very similar with a large amount of 1N2K cells, indicating that the population was progressing through S phase. After 3 hours the peak was tightly centred on 4C (with a small peak at 2C and almost no intermediate signal) and 2N2K cells were observed by DAPI staining, indicating that M phase was occurring. At 4 and 5 hours the 4C peak reduced and the 2C peak increased as cells underwent cytokinesis, with a corresponding increase in 1N1K cells. Finally, 6 hours after release the flow cytometry signal covered the range between 2C and 4C and cells from all stages were abundantly observed by DAPI staining.

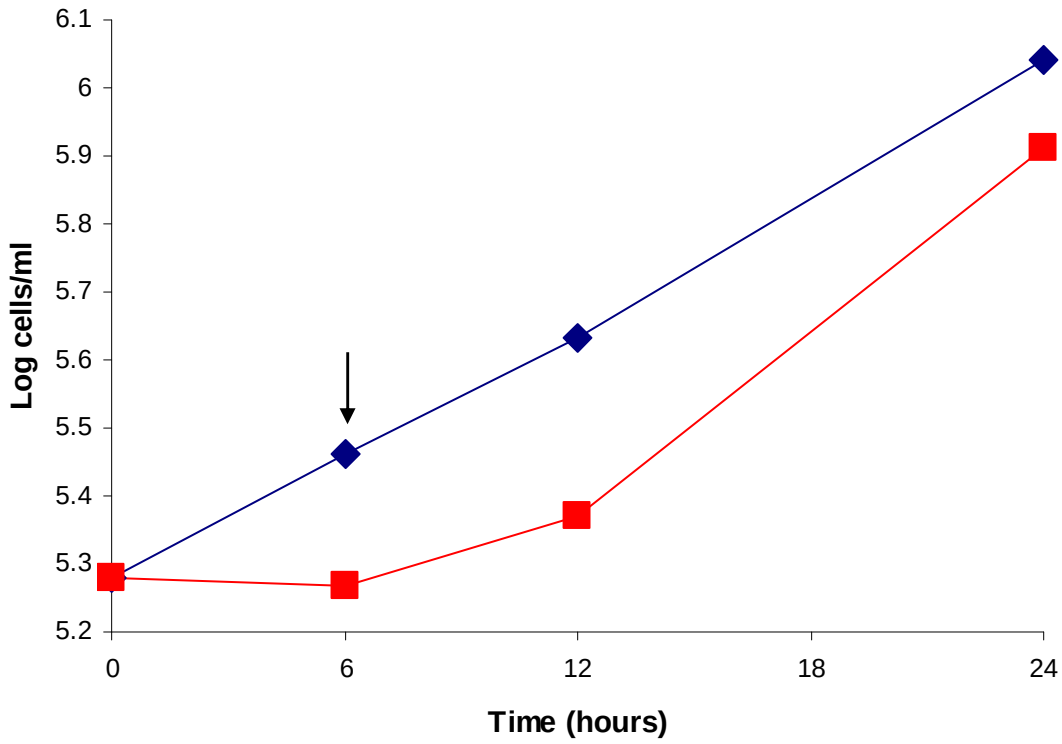

Figure 8

Cumulative growth curves of untreated (♦) and HU treated (■) BSF cells. Arrow shows point at which HU was removed.

1N2K cells can be in S, G_2 or early mitosis phases, so to examine the cell cycle position of the HU treated 1N2K cells more precisely cells were examined for the presence of a mitotic spindle using immunofluorescence with the KMX antibody, which recognises β tubulin (Birkett *et al*., 1985). 1N2K and 2N2K cells were also examined similarly 3 hours after release, based on the data discussed above, to check for mitotic spindles (Fig. 11 and Fig. 12). No spindles were seen in the 1N2K cells which accumulated after 6 hours HU treatment, showing that they had not yet entered M phase. By 3 hours after release from HU, 40% of 1N2K and 60% of 2N2K cells had spindles, showing that they were undergoing mitosis. This equates to 34% of the population undergoing mitosis. The remainder of the 1N2K cells were (given the 4C DNA content) likely to be in G_2 phase, with the remaining 40% of 2N2K cells either undergoing or about to start cytokinesis.

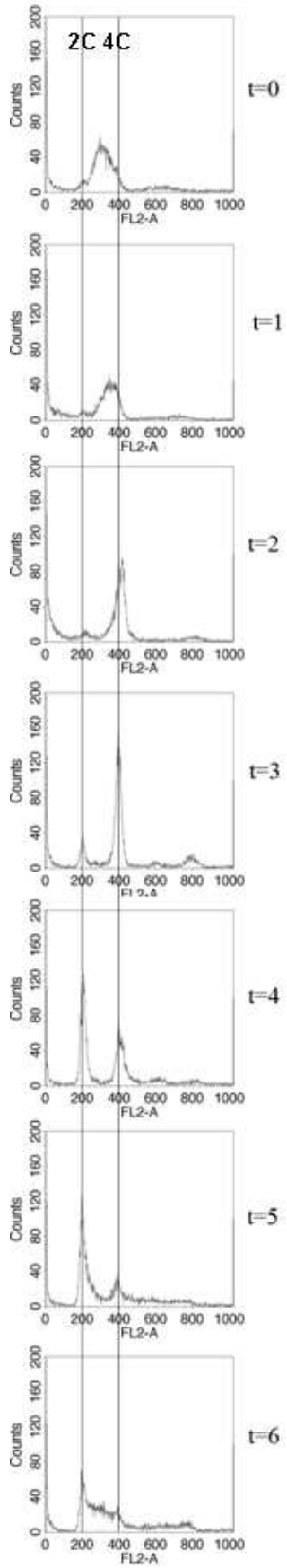

Figure 9: Flow cytometry profiles of DNA content in cells incubated with 10 μg ml^{-1} HU for 6 hours then analysed t hours after release. Vertical lines show position of 2C and 4C DNA content.

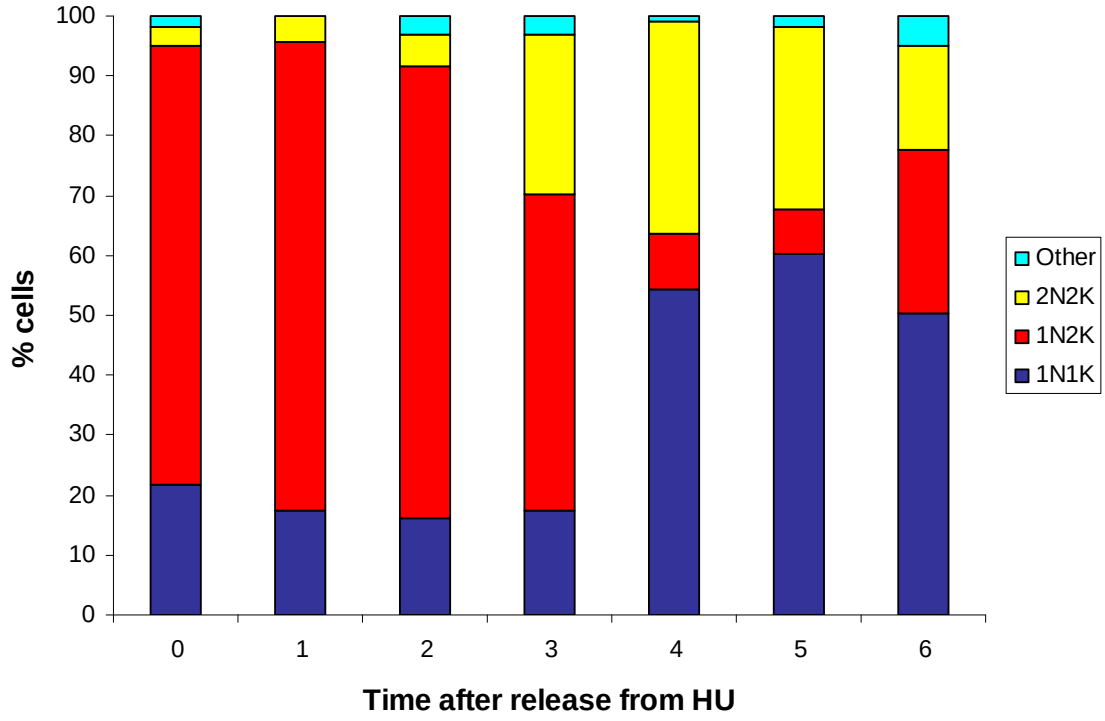

Figure 10
Nucleus (N) and Kinetoplast (K) counts of cells sampled at the same time as Figure 9, as shown by DAPI staining. Other count represents abnormal configurations. n>200 for each time point.

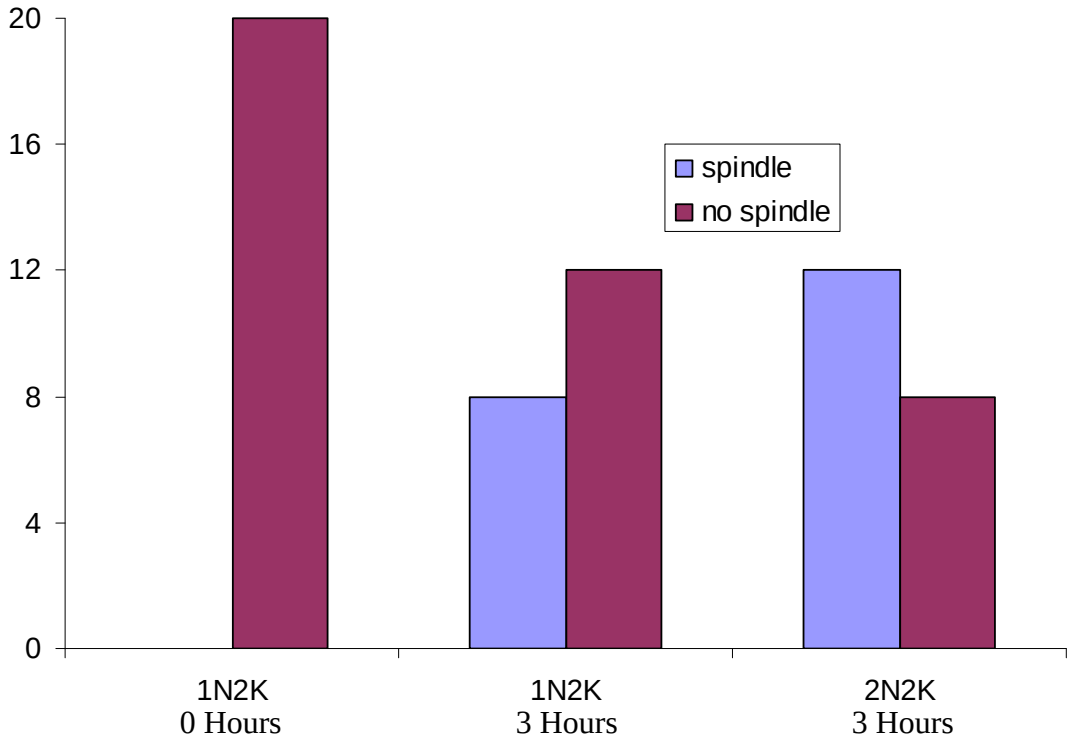

Figure 11
Prevalence of mitotic spindles in 1N2K and 2N2K cells at 0 hours and 3 hours following HU removal, as revealed by immunofluorescence with the KMX antibody. See Fig. 12.

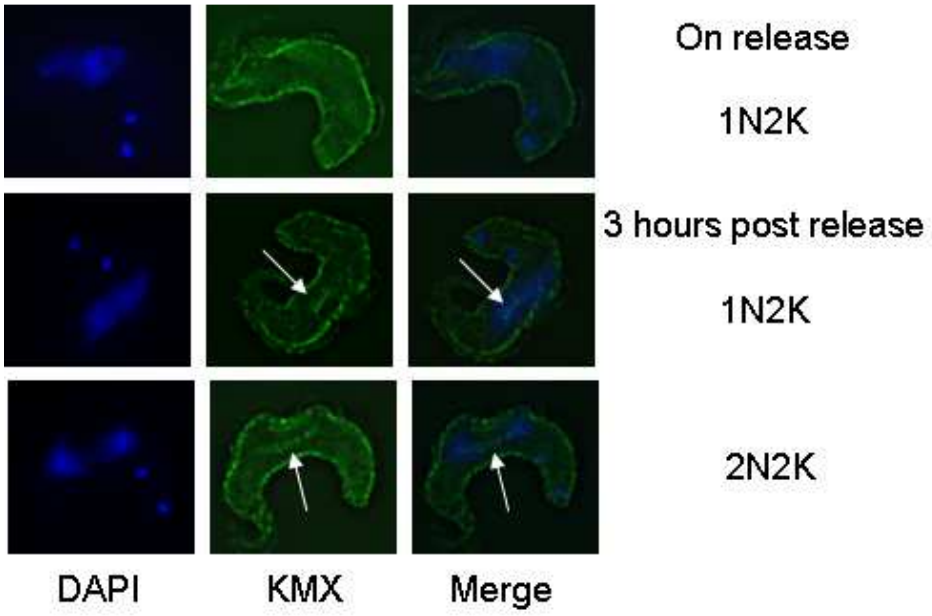

Figure 12

Example images of cells analysed in Figure 11. Left column shows DAPI stained nuclei and kinetoplasts, centre column shows KMX immunofluorescence and right column shows a merge of the previous columns. White arrows indicate mitotic spindles.

Examining protein levels across the cell cycle

Since the cell cycle and DNA damage response are intricately linked (Derheimer and Kastan, 2010) this synchronisation technique presented the opportunity to examine this link in *T. brucei*. To this end, levels of DNA damage response proteins were examined specifically in HU synchronised S phase cultures by western blot, and also more generally by using Difference Gel Electrophoresis (DiGE) to search for proteins upregulated in S phase compared to other phases.

As the procedures available at the time for DiGE with trypanosomes gave better results with PCF rather than BSF cells (R. Burchmore, personal correspondence) the PCF were used for this experiment. HU synchronisation was therefore performed as described in Chowdhury *et al.* (2008), treating the PCF cells with 15 $\mu g.ml^{-1}$ HU for 9.5 hours.

Four independent populations of PCF trypanosomes were split in two, each with half synchronised in S phase with HU and half left to grow asynchronously (Fig. 13). Protein was extracted from whole cell lysates by acetone precipitation. 75 µg of protein was stained with differential dyes and each synchronised/asynchronous population pair was separated by pH (x axis) and loaded onto a 12% tris-glycine SDS polyacrylamide gel for

separation by size (y axis), with a further 500 μg from the 4 populations combined loaded onto a picking gel. No reproducible differences were observed, although 5 protein spots were found to be at least twice as abundant in at least one of the HU-synchronised samples compared with the unsynchronised samples (Table 4 and Fig. 14), and these were identified by mass spectrometry. Three of the samples were identified as β tubulin, heat shock protein 70 and either the 60s ribosomal subunit or elongation factor 2, with the remaining two samples giving no signal. Unfortunately, as these are such abundant proteins few conclusions can be drawn, especially given that these potential changes in abundance were not universally observed.

Prep Gel Spot No.	Gel A	Gel B	Gel C	Gel D	ID
1580	1.87	2.57	1.34	1.34	No ID
1679	1.56	2.12	1.12	1.30	HSP70
1799	1.60	2.21	1.23	1.20	β tubulin
1891	1.71	2.01	-1.17	1.08	EF2 or 60s
1615	2.12	2.18	Not Found	1.44	No ID

Table 4: Relative amounts of protein in 4 DiGE gels as determined by spot intensity, negative integers indicate unsynchronised sample contained the most protein, positive integers indicate synchronised sample contained the most protein.

To ask if changes in repair-associated proteins might occur after synchronisation, but were not at a level detectable by the above approach, western analysis was next undertaken. Affinity purified antibodies were available for two proteins involved in homologous recombination, Rad51-3 and Rad51-4 (Dobson, 2009), and so these proteins were examined by western blot from BSF cells after synchronisation and release from HU (Figure 15 and 16). Both western blots showed bands 10 kDa larger than those reported in Dobson (2009); however, these were the only bands seen on each blot, suggesting that the proteins have migrated differently in the different gel systems used (20% Bis-Tris here, versus 10% SDS-PAGE in Dobson (2009)). No clear changes in abundance or migration were observed, indicating that these proteins do not change in expression during the cell cycle or in response to HU, and that any putative changes in post-translation modification (such as phosphorylation) are insufficient to be detected by size changes in these conditions, if they occur at all.

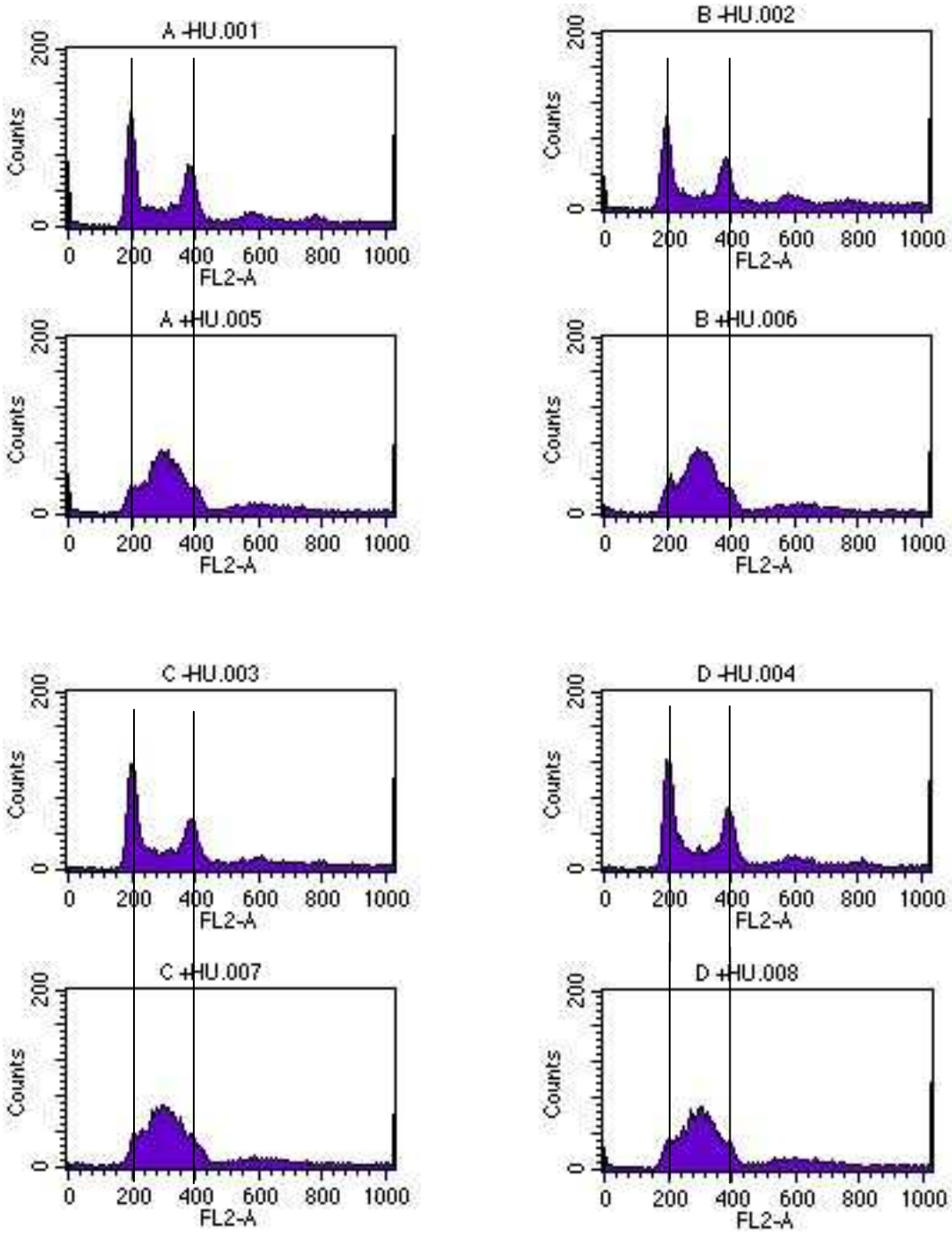

Figure 13: Flow cytometry profiles of DNA content of synchronised and asynchronous (+/- HU) populations of PCF cells. 2C and 4C DNA content are marked by lines.

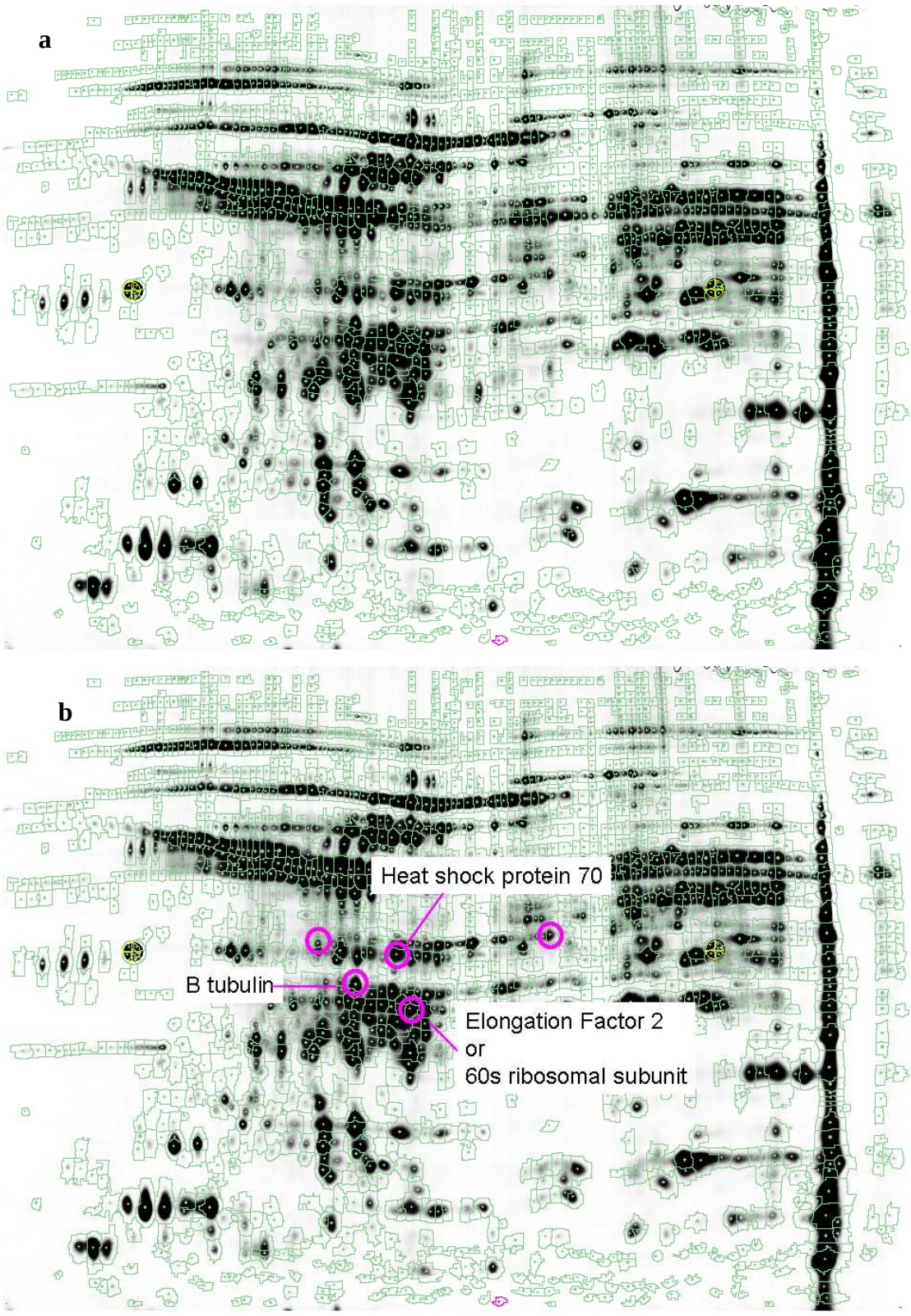

Figure 14: Original (a) and marked (b) 2D picking gel of whole cell protein (all samples combined) from 427 PCF *T. brucei* separated by pH (x axis) and size (y axis). Circles indicate protein spots which had changed by at least 2x in abundance in at least one analysis gel. Identified proteins are marked. (See Table 4, p44.)

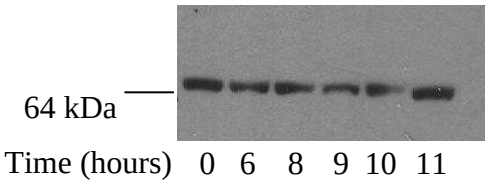

Figure 15:
Western blot with anti-Rad51-3. Time starts from addition of HU, ie. 0 hours unsynchronised population, 6 hours S phase population and removal of HU, 8 hours G_2/M phase population, 9 hours M phase/cytokinesis, 10/11 hours G_1 phase moving into S phase. Compare with DNA content profiles from Fig. 6. Predicted size of Rad51-3 is 54.5 kDa.

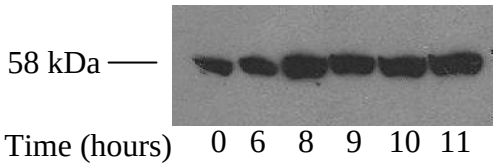

Figure 16:
Western blot with anti-Rad51-4. Time starts from addition of HU, ie. 0 hours unsynchronised population, 6 hours S phase population and removal of HU, 8 hours G2/M phase population, 9 hours M phase/cytokinesis, 10/11 hours G1 phase moving into S phase. Compare with DNA content profiles from Fig. 6. Predicted size of Rad51-4 is 47.7 kDa.

Discussion

In a manner analogous to that reported in Chowdhury *et al*. in the PCF, 10 $\mu g.ml^{-1}$ HU caused an S phase block in BSF parasites, which greatly slowed progression through nuclear S phase, but did not completely halt it. Kinetoplast replication was not obviously affected. As Chowdhury *et al.* speculate, this may be due to different K_m values between nuclear and kinetoplast polymerases, or perhaps the smaller amount of DNA in the kinetoplast compared to the nucleus enabled it to finish replication before the cellular pool of dNTPs was exhausted. It seems significant that 6 hours was the optimal incubation time for HU treatment, as this is also roughly the doubling time for the culture used (calculated as 5.9–6.1 hours).

This correlates well with the hypothesised mode of action for HU (Liermann *et al*., 1990), as the majority of cells should begin DNA replication within this time, allowing the lack of dNTPs to take effect and cause the cells to collect in S phase. Additionally, 6 hours is half the exposure time used in a previous study, which concluded that HU is too toxic for use as a synchronisation tool in trypanosomes (Mutomba and Wang, 1996).

The kinetoplast, spindle and nucleus were studied during and after HU treatment; however, other organelles were not examined. Although nuclear S phase was dramatically retarded other organelles and cellular processes may not be equally affected. Similarly, unwanted downstream effects cannot be ruled out, either from HU or as a consequence of the stalled S phase. The use of minimal amounts of HU for the shortest effective time should minimise any of these non-specific effects, but cell cycle stasis for other organelles and cellular processes cannot be assumed.

In addition to providing a significant enrichment for S phase this technique was also able to provide populations enriched for G_2 and M phases of the cell cycle. It is likely that by modifying the timing HU treatment could be fine tuned to provide more perfect enrichments; however, this will depend largely on the generation time of the specific culture being treated. The only cell cycle stage this procedure has difficulty enriching for is G_1, as the synchronisation loses cohesion as the population reaches the point of division. This may be due to lesions caused by collapsed replication forks formed when replication stalls. The number of these per cell will be largely random, which will give a range of times before cells can fully repair their DNA and pass any checkpoint the damage initiates. It could be possible to reduce this by further optimising the time and concentration of HU

applied, but it seems unlikely that this technique will be as useful for the production of G_1 cells.

The behaviour of cells under HU is of further value to this project, as HU has been shown to induce activation of ATR in other organisms (Ward and Chen, 2001) and would provide another way to analyse *ATR* RNAi cell lines for DNA damage response-related phenotypes (see Results 2). Both ATM and ATR have been implicated in the recovery of collapsed replication forks (Trenz *et al*., 2006), which may provide a way to test the hypothesis that collapsed replication forks prevent synchrony persisting through cytokinesis by searching for ATM/ATR foci after HU treatment in tagged cell lines. If collapsed replication forks are present they could be expected to cause foci of these proteins.

The statistical power of the DiGE experiment was compromised by a mistake in dye application preventing the use of standards to normalise the analysis gels. However, even within individual gels no difference greater than a 2.57 ratio was found between the synchronised and unsynchronised samples. This suggests that either there are very minor differences in protein expression between cell cycle stages, or perhaps more likely that any differences are in proteins not found among the 2000 most abundant in the whole cellular fraction. One way to address this would be to take fractions of the cellular protein (such as the nuclear fraction) and analyse these, as this would allow examination of less abundant proteins. It may also be more productive to compare S phase with a specific other cell cycle stage, rather than an unsynchronised population which contains a proportion (albeit lesser) of cells in S phase already.

Although neither of the 2 proteins examined specifically showed any difference in expression across the cell cycle this is a very small sample of proteins tested. For example, there are 2 further paralogues, Rad51 itself and BRCA2. Further tests should also include a loading control of a protein unlikely to be affected by the cell cycle stage.

Results 2

RNAi of *ATM* and *ATR*

Generation of RNAi cell lines

RNAi cell lines were created for both *ATM* and *ATR* in procyclic form 427pLEW13pLEW29 and bloodstream stage 427pLEW13pLEW90 T. brucei cells (Wirtz et al., 1999). An *ATM* fragment from bases 5 to 597 of the ORF was PCR-amplified using the primers OL2763 and OL2757, as detailed in table 1. Likewise an *ATR* fragment from bases 4245 to 4657 was PCR-amplified using primers PR160 and PR161. The *ATR* fragment was then subcloned into p2T7/GFP (LaCount et al., 2000) using *Sac*II and *Xho*I to give pHG146, while the *ATM* fragment was subcloned with *Bam*HI and *Xho*I to give pHG13 (Fig. 18 and Table 2). pHG13 and pHG146 were then linearised with *Not*I and transfected into procyclic form 427pLEW13pLEW27 and bloodstream stage 427pLEW13pLEW90 using the AMAXA nucleofector. Clonal cell lines were produced using 2.5 µg.ml-1 phleomycin as the selective drug on a serial dilution to 1:1000. In the BSF, 4 clones were recovered for *ATM* and 3 for *ATR* RNAi. In the PCF, 4 clones were recovered for *ATM* and 5 for *ATR* RNAi.

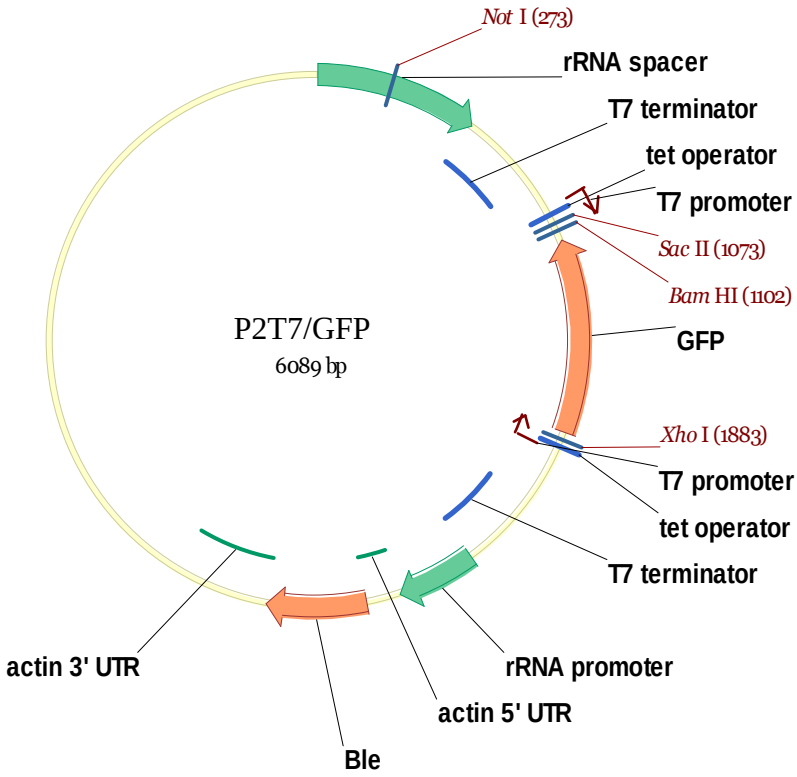

Figure 17 (part 1) Parent plasmid p2T7/GFP and (on the next page) plasmids for RNAi of *ATM* (pHG13) and *ATR* (pHG146). *Not*I restriction site for linearisation is shown. rRNA spacer is present, causing constructs to integrate into rRNA spacer region.

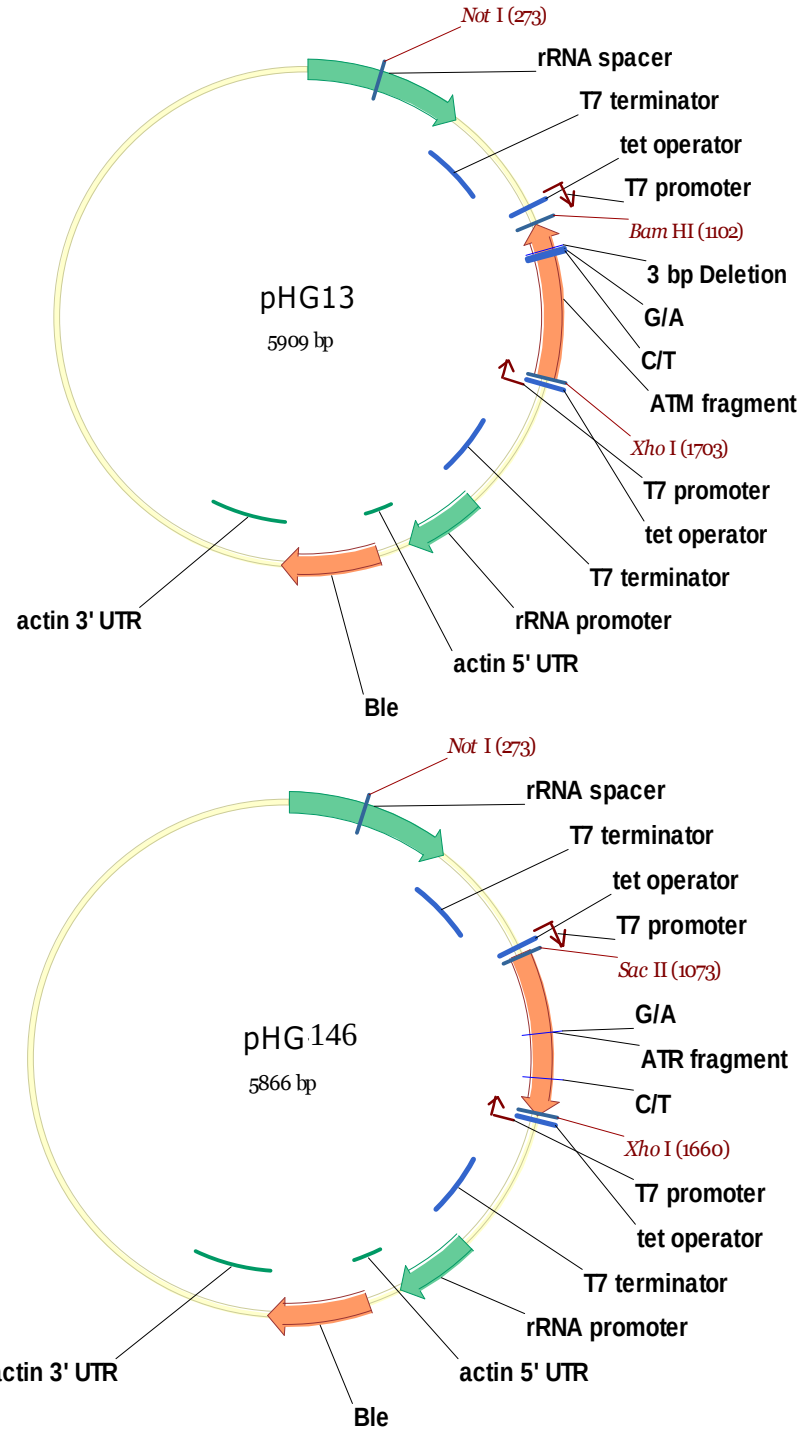

Figure 17 (part 2)

Analysis of effect of *ATM* and *ATR* RNAi

Procyclic form parasites were grown to 10^6 cells.ml^{-1} and RNAi induced with 1 µg.ml^{-1} tetracycline. Cultures were diluted when necessary to 1-5 x 10^6 cells.ml^{-1} with fresh medium to keep below 2 x 10^7 cells.ml^{-1} and tetracycline levels maintained and counts multiplied by this dilution factor to simplify graphs (Fig. 18). Similarly, RNAi in BSF parasites was induced at 1-5 x 10^5 cells.ml^{-1} and diluted to remain below 1x 10^6 cells.ml$^{-.1}$ (Fig. 19).

Procyclic cell lines showed a weak growth phenotype after approximately 8 days of RNAi induction for both *ATM* and *ATR*, with growth being reduced but not halted after this time (Fig. 18). None of three BSF *ATR* RNAi clones showed any growth phenotype after 6 days, but a strong growth phenotype resulting in death within 5 days was observed in 2/4 clones for BSF *ATM* RNAi (Fig. 19), with the remaining two clones showing no response to tetracycline. Although the BSF clones were analysed for less time than the PCF the shorter doubling time of the BSF cells means that more generations were analysed.

The BSF *ATM* RNAi clones that displayed a growth defect were analysed in more detail with samples taken for nuclei/kinetoplast analysis by DAPI staining and DNA content analysis by flow cytometry. Although not consistent, DAPI staining (Fig. 20, see Fig. 21 and 22 for example images) showed there to be a general decrease in the proportion of 1N1K count. This was visible from the first point of measurement after 12 hours of induction and increased by 18 hours, although the 15 hour measurement showed a small increase in 1N1K cells, which may suggest that some of the 2N2K or abnormal cells managed to divide after some delay. Division of cells with abnormal N and K counts may also account for the increasing numbers of 2N1K and other non-standard cell types seen over time. As incomplete (0NxK or xN0K, where x<3) cell types did not increase then the 2N1K cells can only have been produced through either re-replication of the nucleus, but not kinetoplast, or division from cells with N and K counts greater than 2N2K. 2N2K cells were further subdivided into those with and without a visible furrow, and those at the point of abscission (1N1K-1N1K) as the RNAi induced cell population initially seemed to have more cells in abscission than the uninduced. This hypothesis was not borne out by the DAPI counts; however, there was a small increase in cells with 3 or more cell bodies (>= triplets), apparently trapped at the point of abscission.

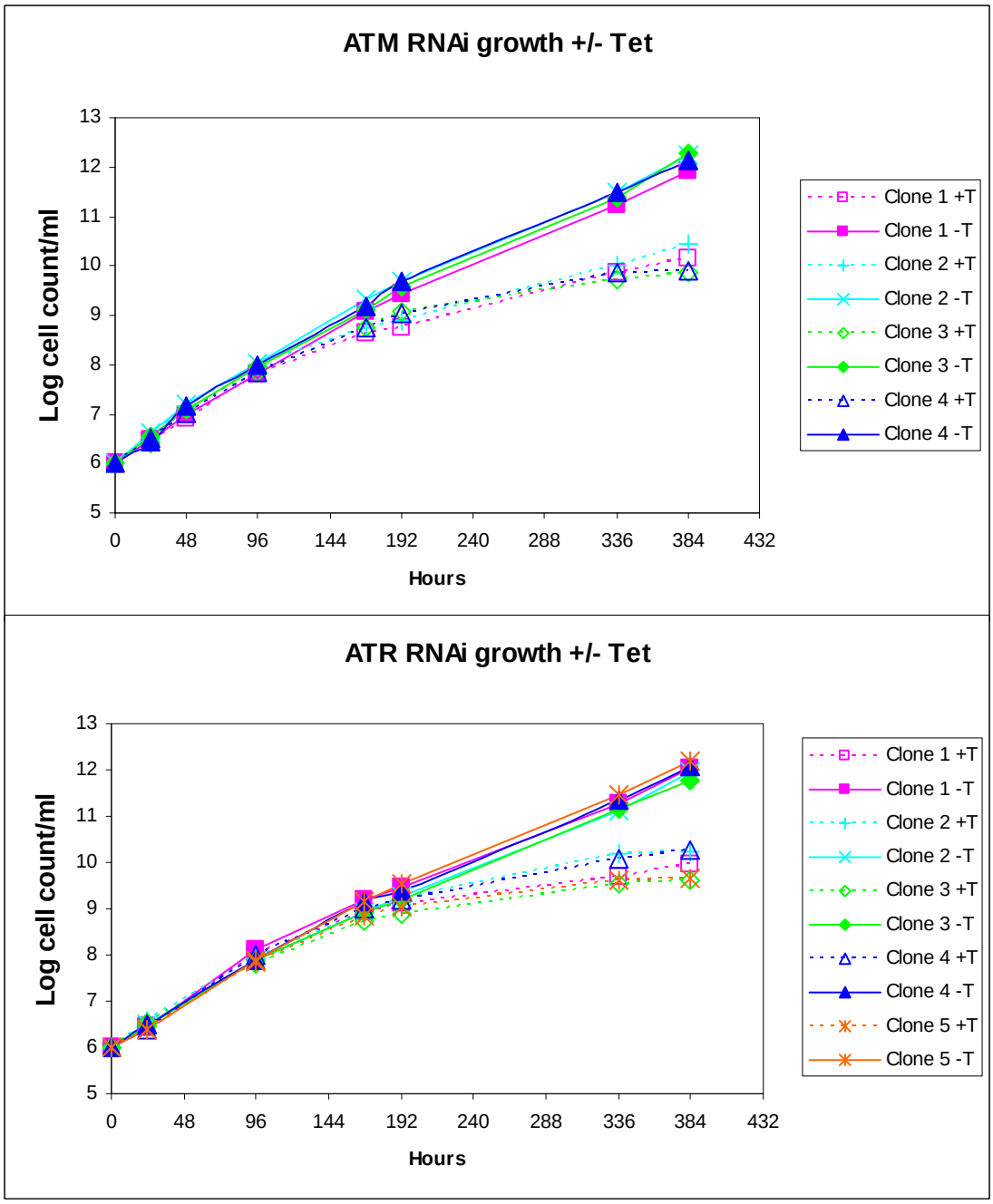

Figure 18
Cumulative growth curves for PCF *ATM* and *ATR* RNAi cell lines induced/uninduced (+/-) with 1 μg.ml^{-1} tetracycline (T). Each clone is an individual transfectant.

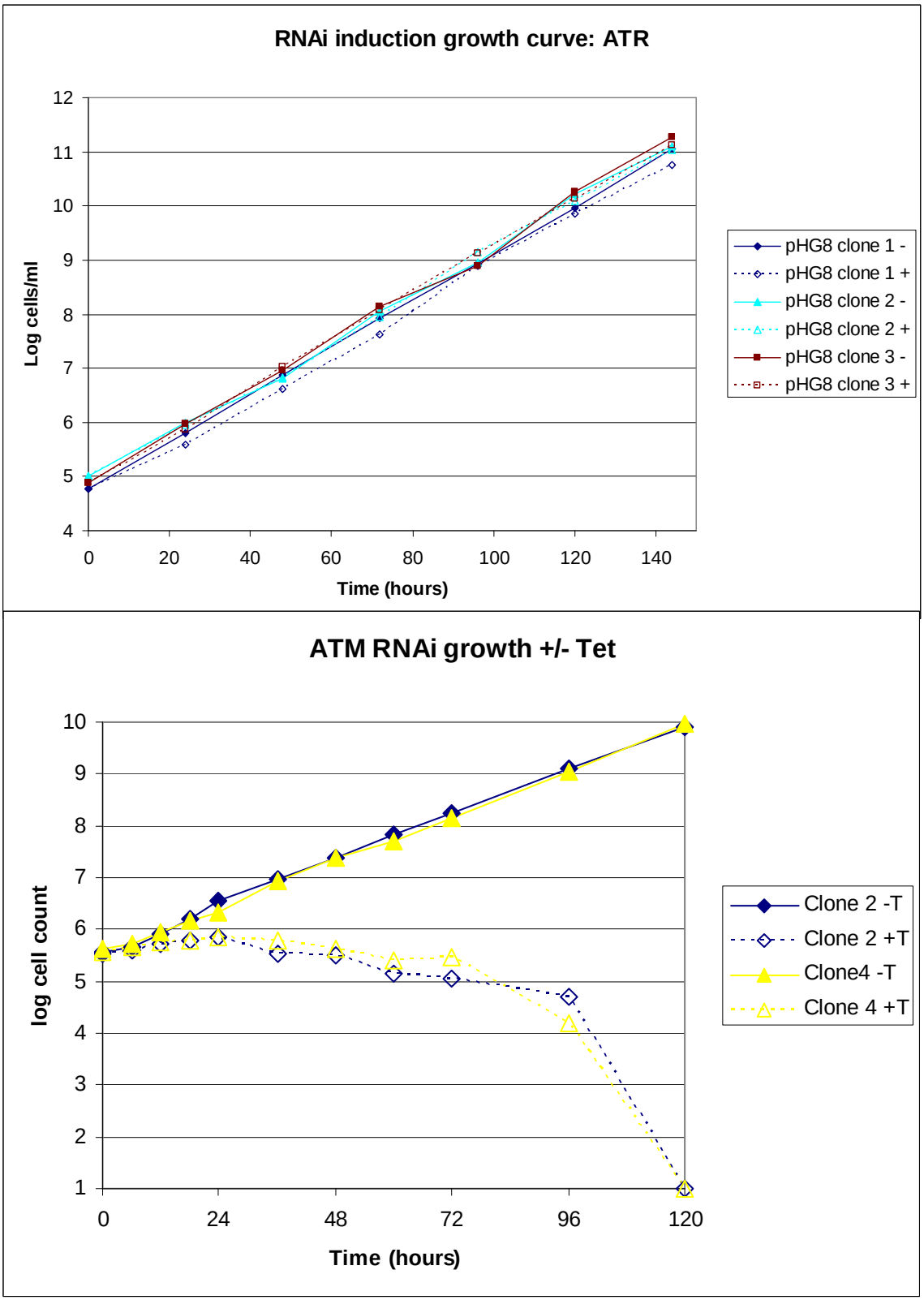

Figure 19 (part 1)**:** Cumulative growth curves for BSF *ATM* and *ATR* RNAi cell lines induced/uninduced (+/-) with 1 µg.ml^{-1} tetracycline (T). Each clone is an individual transfectant. Clones 1 and 3 from the *ATM* RNAi are shown on the next page.

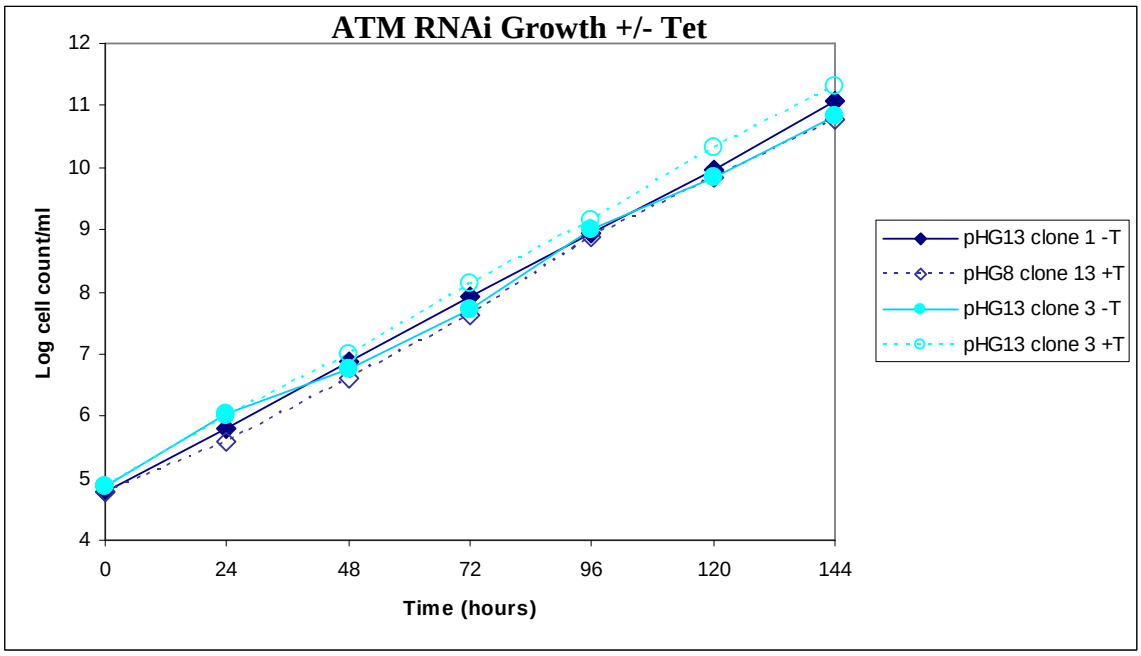

Figure 19 (part 2)

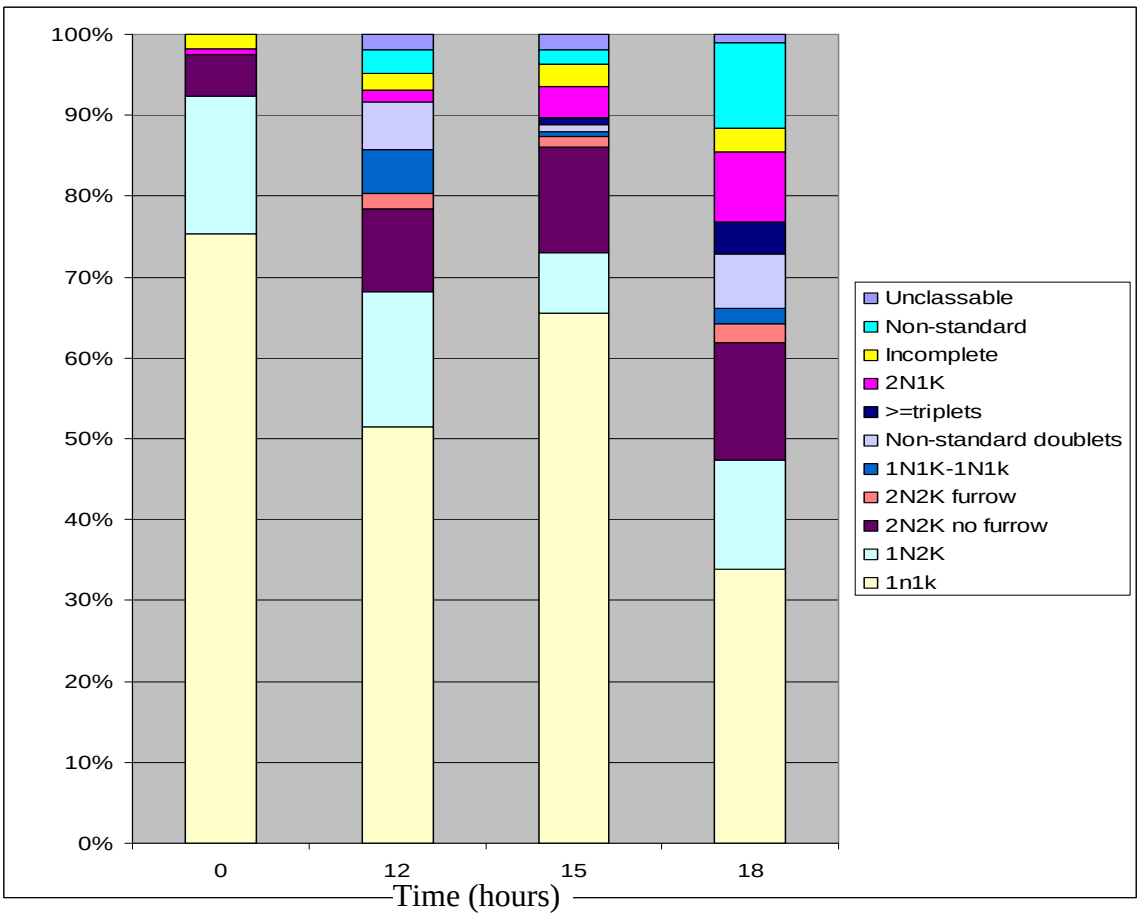

Figure 20
Proportion of cells with given nucleus (N) and kinetoplast (K) counts from DAPI stained BSF *ATM* RNAi clone 4 cells. Time is hours post RNAi induction with 1 μg.ml^{-1} tetracycline. 2N2K cells were further divided into those before furrow ingression ("no furrow"), those undergoing furrow ingression ("furrow") and "doublets" where the furrow had completed progression and the cells were in abscission ("1N1K-1N1K"). Non-standard doublets includes all cells in abscission which were not 1N1K-1N1K, eg. 1N2K-1N2K. >=triplets refers to cell with three or more cell bodies apparently trapped at the point of abscission. "Non-standard" includes single bodied cells with N and K counts which do not match any of the "normal" counts (1N1K, 1N2K or 2N2K). "Incomplete" and "2N1K" are subsets of non-standard, with incomplete cells lacking either a nucleus or kinetoplasts. 2N1K cells were shown separately as the most common non-standard configuration. "Unclassable" cells contained so many nuclei and/or kinetoplasts that they were uncountable. These categories were chosen to distinguish between errors in organelle distribution and errors in abscission.

Similar to the decrease in 1N1K cells, the 2C peak in the flow cytometry analysis (Fig. 23) showed a decrease by 6 hours which continued until 24 hours. Meanwhile there was an increase at roughly 8C (equivalent to 4 fully replicated sets of DNA) corresponding to the 2C decrease. The 4C peak remained broadly stable, however, not reflecting the increase in 2N2K cells seen by DAPI staining. This suggests that each nucleus in many of the 2N2K cells may have more than the standard complement of DNA. The growth phenotype may

therefore be due to cells having difficulty preventing DNA rereplication and performing normal DNA segregation and cytokinesis.

The BSF *ATM* RNAi clones with growth phenotypes were examined first to attempt to shed light on the gene function. Analysis by DAPI staining and flow cytometry was not completed for the other BSF or PCF cell lines, although this would be a sensible place to continue the analysis.

To examine whether the DNA damage response functions normally with reduced levels of ATM, RNAi was induced in the BSF cells and incubated with increasing concentrations of the alkylating agent methyl methanesulfonate (MMS) (Fig. 24). Although MMS does not directly produce DSBs HR is still important in the cellular response to MMS (Lundin *et al*., 2005), and therefore if the DNA damage response was compromised then lower concentrations of MMS could be expected to have an effect on growth rates. Although the culture treated with 0.3 $\mu l.ml^{-1}$ MMS showed a reduction in growth in uninduced cell populations within 24 hours, the growth rates for all induced cultures became negligible almost immediately, with no discernible difference between cultures containing different MMS concentrations. This suggests that either there is no effect on growth rate of *ATM* RNAi BSF cells by MMS or the effect is completely hidden beneath the already large growth impairment phenotype post-RNAi.

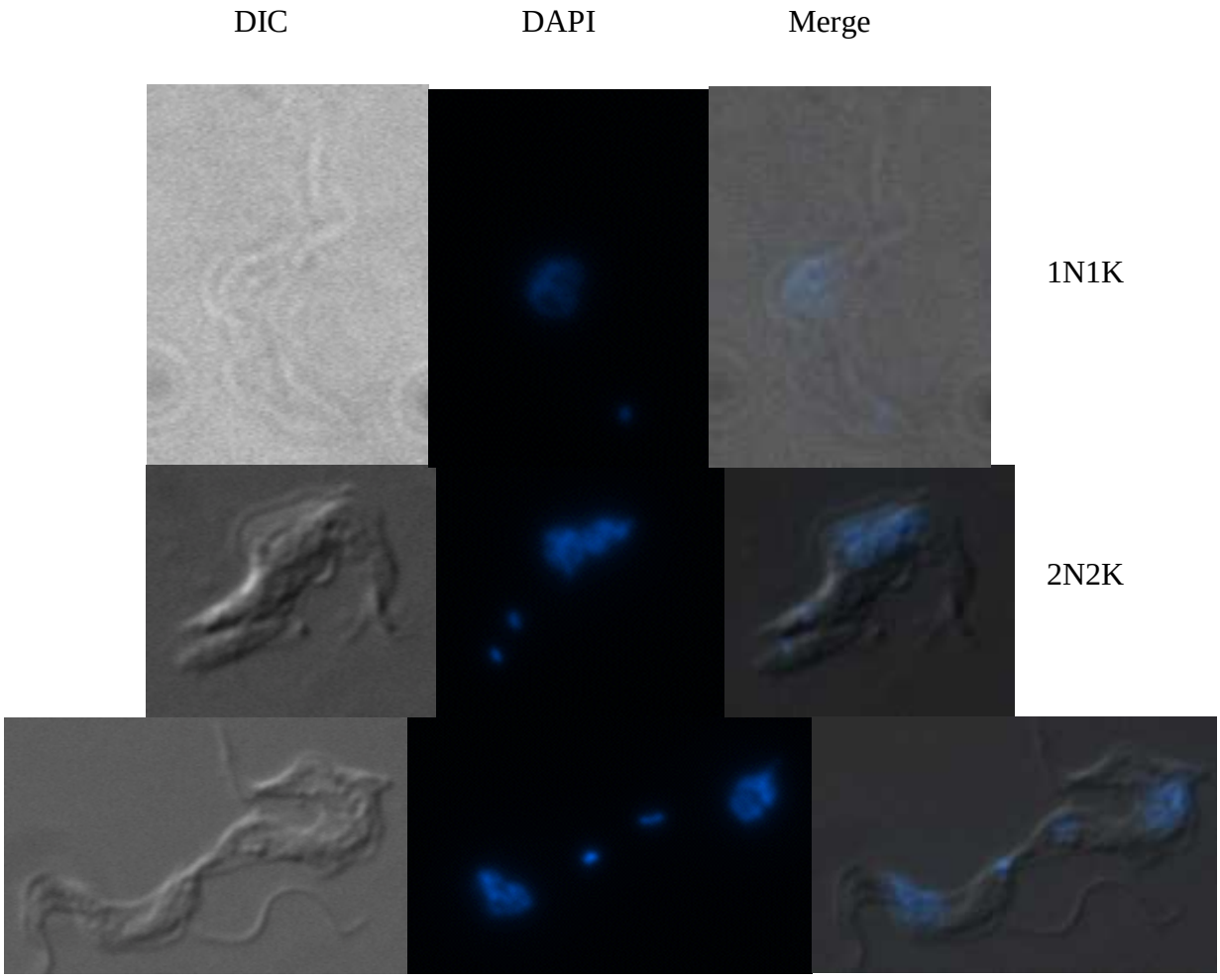

Figure 21

DIC, DAPI stained and merged example images for normal cell types shown in the previous figure, taken from various time points.

Verification of knockdown:

Probes for northern blot hybridisation were produced (using primers PR287 and PR239 for *ATM*, PR300 and PR81 for *ATR* and β tub f and β tub r for β tubulin as a loading control, see Table 1) for regions outside those used to produce the RNAi fragments, and RNA recovered from 10^8 cells induced with 1μg.ml^{-1} tetracycline for 18 hours using the Qiagen RNeasy kit on a Qiacube automated system to ensure even treatment of samples. 5 μg of each RNA sample were digested with Ambion RNase free DNase I. 1 μg of each sample was then separated by electrophoresis on a 1.5% agarose gel containing 2.2M formaldehyde and transferred onto nylon membrane by capillary transfer overnight. Hybridisation with radioactive probes was carried out as described in the materials and

methods section. The northern blots were inconclusive, however, as a discrete band could not been seen for either product (Fig. 25).

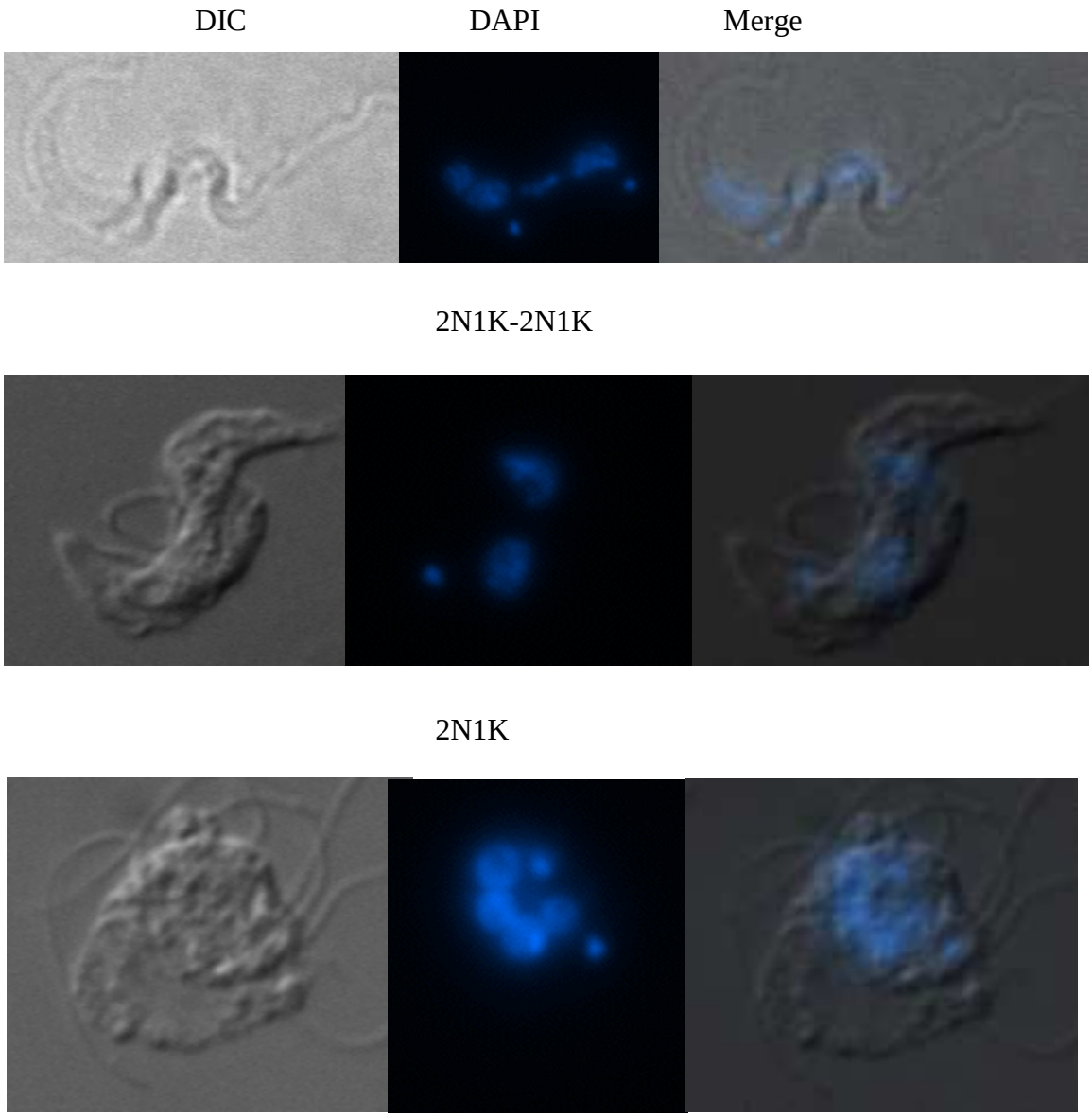

Figure 22
DIC, DAPI stained and merged example images for abnormal cell types shown in Figure 4, taken from various time points.

To give an alternative method of establishing whether knockdown had occurred native tagging vectors were constructed for ATR and ATM, called pHG104 and pHG105 (see Fig. 26), using long primer PCR to amplify a Neomycin resistance cassette and mCherry tag with 70bp of the *ATR* 5'UTR and ORF, respectively (PR67 and PR68, see Table 1). Likewise, a Blasticidin resistance cassette was amplified with 70bp of the *ATM* 5' UTR and eGFP with 70bp of the *ATR* ORF (PR69 and PR70, see Table 1). These were then

cloned into the Strataclone vector pSC-B using the Strataclone blunt ended cloning kit to produce pHG104 (for *ATR*) and pHG105 (for *ATM*). After being excised from these vectors with *Eco*RI, transfected into *T. brucei* and integrating into the endogenous *ATM* or *ATR* locus, this will enable expression of mCherry-*ATR* and GFP-*ATM*. A polyclonal anti-GFP antibody (Abcam6556) detected enough signal to demonstrate knockdown of ATM at the protein level in both clones of the BSF *ATM* RNAi cell line which gave a growth phenotype (Fig. 27). All induced samples can be seen to have less intense bands than the corresponding uninduced sample, except for Clone 2 105C. However the loading control (Fig. 27b) shows that the Clone 2 105C tetracycline induced sample contains more protein than the uninduced. In none of the mCherry-ATR clones could protein be detected in this approach (data not shown).

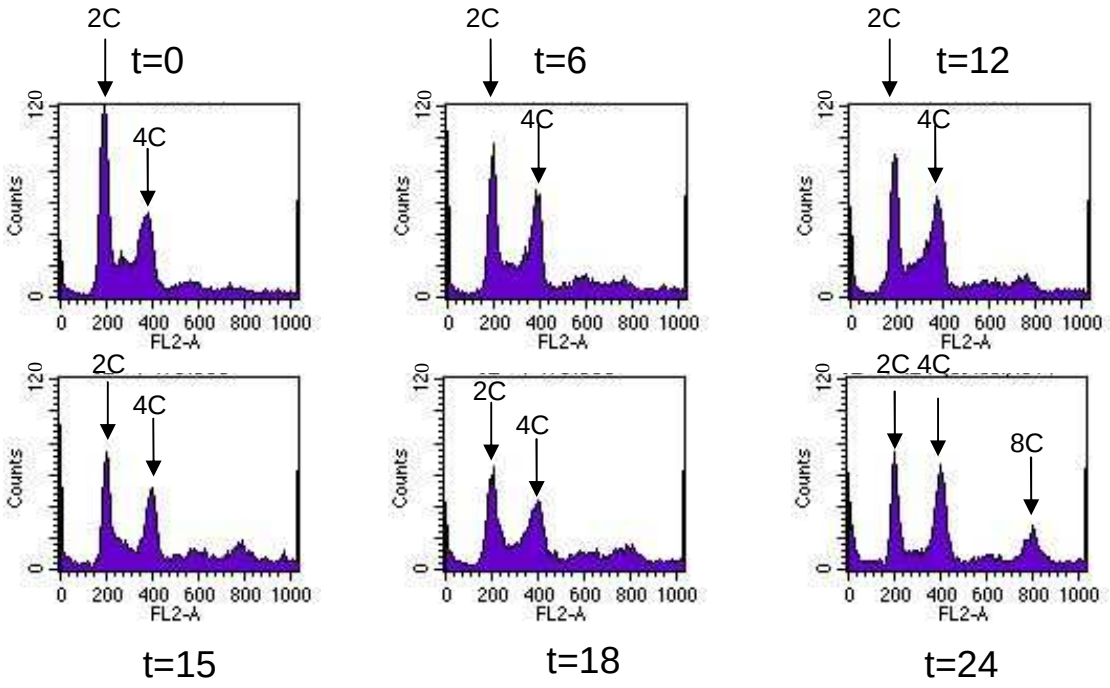

Figure 23
Flow cytometry analysis of propidium iodide stained BSF *ATM* RNAi clone 4 cells. Time (t) is hours post RNAi induction with 1 μg.ml^{-1} tetracycline.

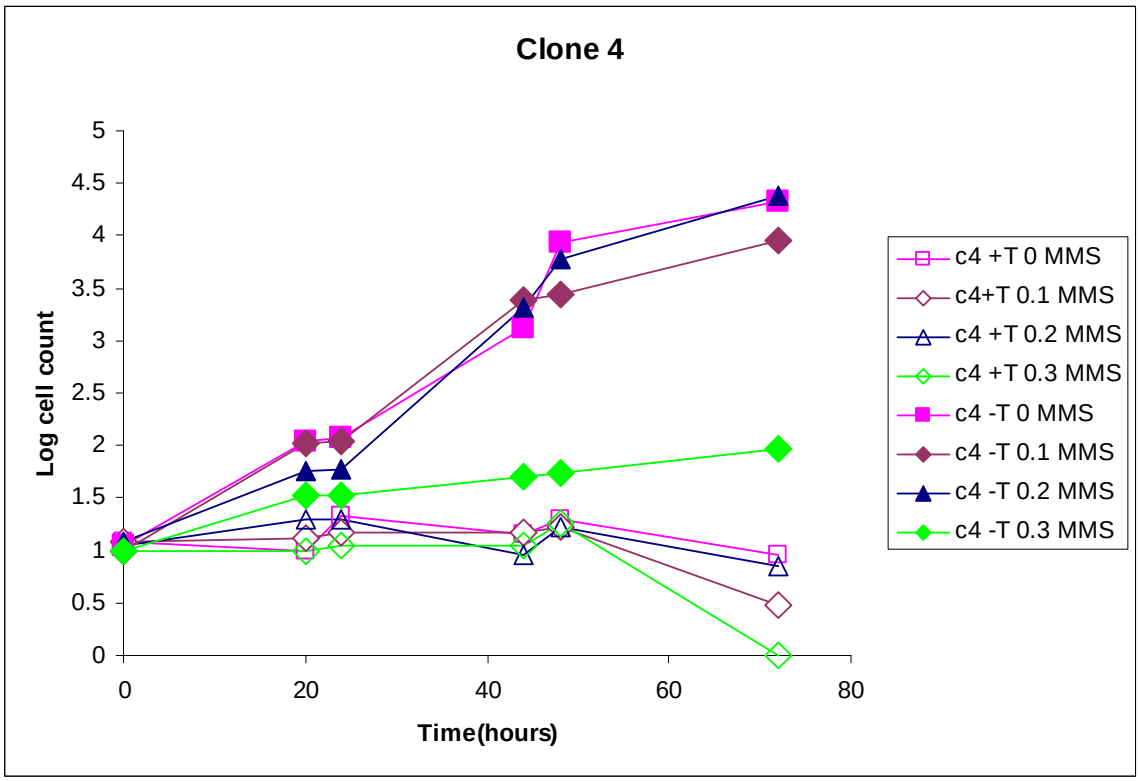

Figure 24: Growth curve of BSF *ATM* RNAi clone 4 induced/uninduced (+/-) with 1 $\mu g.ml^{-1}$ tetracycline (T) and incubated 0 to 0.3 $\mu l.ml^{-1}$ of MMS.

Discussion

RNAi cell lines were produced for both *ATM* and *ATR* in PCF and BSF *T. brucei*. The PCF cell lines all showed a minor, non-lethal growth phenotype after RNAi induction. In the BSF, *ATR* RNAi cell lines showed no growth phenotype after induction, while *ATM* RNAi lines showed a strong growth phenotype leading to death. This is not unexpected, as in other organisms either *ATM* or *ATR* have been shown to be essential, with *ATR* knockout cell lines leading to embryonic lethality in mammals (Brown and Baltimore, 2000; Gilad *et al*., 2010) and ATM being essential in *Saccharomyces cerevisiae* (Brush *et al*., 1996). *ATR* may either be not essential in the BSF, or simply not depleted sufficiently by the RNAi to have an effect. As the level of knockdown has not been established in the two *ATM* RNAi clones not to show a growth phenotype it cannot be stated whether this lack of response is due to different levels of knockdown, a complete failure to respond to induction, perhaps by some failure of some part of the RNAi system, or a different response to similar levels of knockdown.

It could be expected that DNA repair proteins would be more essential in the procyclic form, as this lifecycle stage has active mitochondria (Fenn and Matthews, 2007),

implicated in the production of reactive oxygen species which may damage DNA (Vendelbo and Nair, 2011), while mitochondrial activity is largely absent in BSF parasites (Bringaud *et al*., 2006). This does not appear to be the case here given the lethal phenotype is in the BSF. However, DSBs may still be central to the difference between *ATM* RNAi in BSF and PCF stages. It has been shown that DSBs occur naturally and specifically at the active VSG expression site in the BSF and that this is involved in antigenic variation (Boothroyd *et al*., 2009). Boothroyd *et al*. did not examine whether this DSB formation is repressed in the PCF, but as it did not occur at inactive expression sites a repression mechanism must exist. ATM could therefore be essential for repairing this increased load of DSBs in the BSF, accounting for the difference in growth phenotypes. This can only be an extremely tentative hypothesis in the absence of data about the level (if any) of *ATM* knockdown in the PCF compared to the BSF.

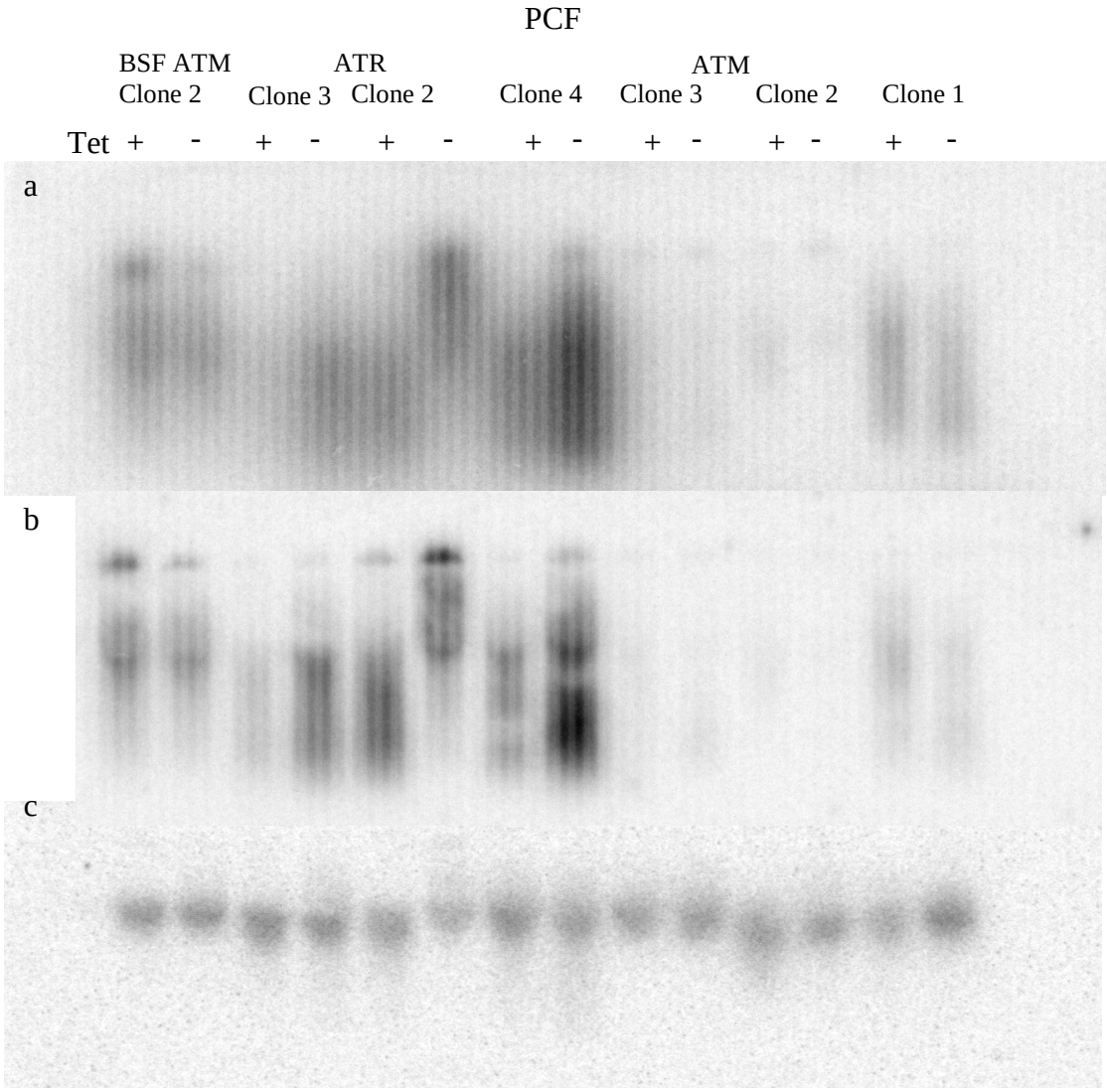

Figure 25
Northern blot of RNA extracted from BSF and PCF *ATM* and *ATR* RNAi cell lines. Section a shows blot probed for *ATM*, section b shows blot probes for *ATR* and section c shows β tubulin controls. RNA was harvested from 10^8 cells treated with +/- 1 μg.ml^{-1} tetracycline (Tet) for 18 hours.

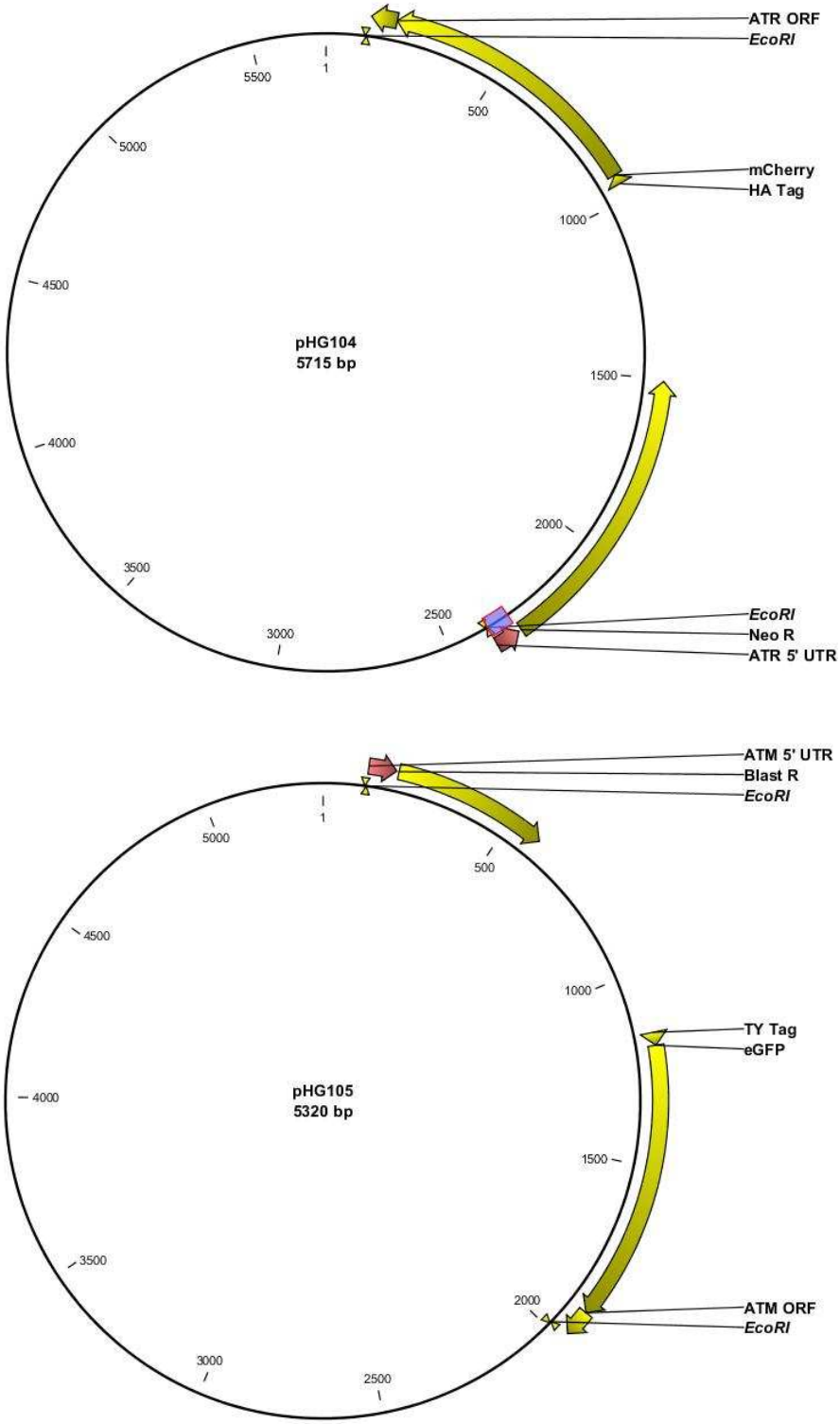

Figure 26: N terminal tagging constructs to produce natively tagged HA:mCherry:ATR and TY:GFP:ATM. *Eco*RI sites to produce linear DNA for transfection are shown.

In the *ATM* RNAi cell lines the disagreement between the increasing 2N2K count by DAPI staining and the lack of increase in the 4C peak by flow cytometry suggests that DNA replication and segregation are not occurring normally. It may be that some of the nuclei actually contain more than the correct amount of DNA, ie. the DNA is being re-replicated before cytokinesis occurs. ATM has been shown to be involved in prevention of DNA re-

replication in other organisms (Truong and Wu, 2011). There was no difference in growth rates in the induced *ATM* RNAi cell lines when treated with different concentrations of MMS, although the higher concentration was enough to reduce the growth rate in uninduced cells. If the decrease in growth rate in the uninduced cells treated with MMS is due to the DNA damage response then the lack of any change in growth rate in the induced cells may be indicative of a lack of DNA damage response. Alternatively the response may be functioning normally but be effectively "invisible" in this experimental setting due to the lack of growth in the induced RNAi line. This could be tested by analysing the DNA content profile by flow cytometry and by counting the nucleus/kinetoplast numbers to detect any differences in the proportions of cells in the various cell cycle stages. If there were a DNA damage response a change in cell cycle stage could be expected, even compared to the unhealthy RNAi induced cells.

In order to determine if the growth defects seen after RNAi induction in the procyclic form cell lines and the lack of growth defect in the BSF *ATR* cell lines are real phenotypic differences caused by decreased levels of these proteins the level of knockdown must be measured in some way. Tagging at the native locus is likely to be the most effective technique given the difficulty encountered here using RNA-based techniques. In addition, single knock out cell lines coupled with native tagging should be performed to check that replacing one copy of the genes with tagged variants does not itself have an effect. Double knockout cell lines may also reveal more, assuming the proteins are not essential. *ATM* is likely to be essential in the BSF given the lethal nature of the RNAi phenotype, but may not be in PCF, which would provide more information about the function of this protein in *T. brucei*. Given that natively tagged cell lines are being produced, a reasonable next step would be to use these to examine the localisation of ATM and ATR under DNA damaging and normal conditions. In several organisms they have been shown to form foci in response to DNA damage (Dubrana *et al*., 2007; Suzuki *et al*., 2006). The use of HU synchronisation in the BSF and PCF may also provide interesting data; for example, as ATR is activated in other organisms in response to HU (Ward and Chen, 2001), an ATR deficient cell may not respond normally to an HU induced replication block.

In summary, knockdown of *ATM* in the BSF leads to a visible reduction in levels of the protein as shown by native locus tagging. This corresponds to a lethal growth phenotype, suggesting that this protein may be essential in the BSF. As levels of knockdown have not yet been demonstrated for BSF *ATR* RNAi or for either *ATM* or *ATR* in the PCF, it cannot be determined whether the phenotypes shown are representative of knockdown. BSF *ATM*

knockdown did lead to apparent problems with DNA re-replication, which is consistent with its function in other organisms, but direct function in DNA damage pathways has not been demonstrated.

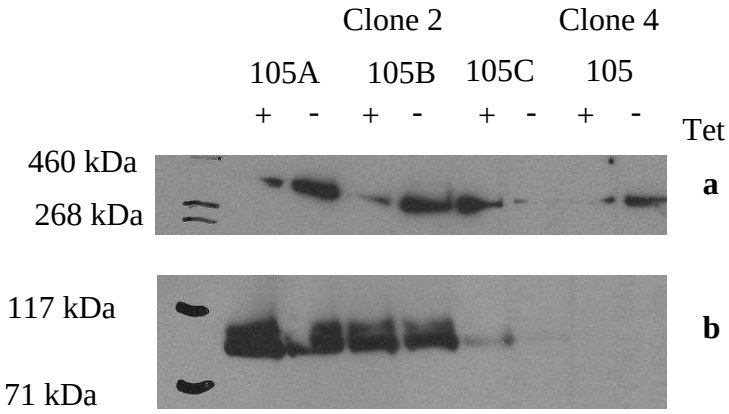

Figure 27

a: Western blot using polyclonal anti-GFP antibody on BSF GFP-*ATM* RNAi cell lines tagged at the native locus and induced with 1 μg.ml^{-1} tetracycline (Tet) for 18 hours or grown normally. 3 independent transfectants were produced for clone 2 (105A, B and C) and one for clone 4.

b: Western blot on same membrane as **a** using anti-OPB antiserum (Munday *et al.*, 2011) for a loading control. Expected size is 80 kDa.

General Discussion

This project has demonstrated a significant enrichment for S phase bloodstream form *T. brucei* using hydroxyurea. Using this technique to provide populations of cells enriched for different cell cycle stages attempts were made to look for variation in the levels of DNA damage response related proteins, both specifically and generally, although no evidence of changes in relative protein levels over the cell cycle was found. RNAi cell lines of two DNA damage response signalling proteins, ATM and ATR, showed a large, lethal growth phenotype for the *ATM* RNAi cell line in the bloodstream stage parasites and a minor growth phenotype in procyclic form parasites for both the ATM and ATR proteins. Knockdown has been demonstrated at the protein level for the *ATM* RNAi cell lines, but not for the remainder. This demonstrates progress towards validation of equivalent functions of the ATM and ATR proteins in *T. brucei* compared with other organisms, but further work is required to test whether these proteins occupy a similarly central role in the *T. brucei* DDR and any possible differences unique to *T. brucei*.

Hydroxyurea synchronisation:
BSF 427 *T. brucei* were treated with 10 $\mu g.ml^{-1}$ HU for 6 hours, resulting in 90% of the cell population stalled in S phase. After release from HU the cells remained reasonably synchronous through G_2/M phase but lost synchrony after cytokinesis. This work was published as Forsythe *et al.* 2009.

Using this technique attempts were made to examine relative levels of DNA damage proteins through the cell cycle, using antibodies against proteins Rad51-3 and Rad51-4 and, more generally, using DiGE to compare an HU synchronised S phase population with an unsynchronised population. Only the procyclic form parasites were studied with DiGE, as at the time procedures had not been optimised for the bloodstream stage as effectively, this is no longer the case (R. Burchmore, personal communication) so in the future bloodstream stage parasites could be studied with DiGE. No differences were found across the cell cycle with either technique. This is somewhat surprising, perhaps, as levels of 430 RNA transcripts have been shown to change through the *T. brucei* cell cycle (Archer *et al*., 2011). However, it may simply be that the DiGE was not sensitive enough to detect proteins which were being regulated differently as it will only register the 2000 most abundant (R. Burchmore, personal communication; also roughly the number of protein spots seen here). Other proteins such as ATM, ATR or BRCA2 may be worth examining directly by western blot, and the natively tagged cell lines for ATM and ATR produced

here could be useful for this. The DiGE may be more sensitive if only certain fractions of the total cellular proteins are examined instead of using whole cell lysate as here, for example the nuclear fraction could be isolated (Rout and Field, 2001). Alternative methods of producing populations enriched for certain cell cycle stages could also be used. S phase was compared with unsynchronised populations here because unsynchronised populations are mostly non-S phase cells, however it may be more effective to use cell sorting techniques (Archer *et al*., 2011; Kabani *et al*., 2010) which seem to be more effective at producing a population in G_1 or G_2/M to produce an alternative population for comparison. No technique for enriching for cell cycle stages is without its drawbacks, so combining the strengths of the techniques in this way may prove fruitful. The procedure developed by Archer *et al.* in particular may provide a technique which affects cells less drastically than HU or the long period of time on ice required for Kabani *et al.*'s vibrant dye based sorting.

RNAi of *ATM* and *ATR*

RNAi cell lines were produced for both *ATM* and *ATR* in PCF and BSF *T. brucei*. The PCF cell lines all showed a minor, non-lethal growth phenotype after RNAi induction. In the BSF, *ATR* RNAi cell lines showed no growth phenotype after induction, while 2 of 4 *ATM* RNAi lines showed a strong growth phenotype leading to death. This is not unexpected, as in other organisms either *ATM* or *ATR* have been shown to be essential, with ATR knockout cell lines leading to embryonic lethality in mammals (Brown and Baltimore, 2000; Gilad *et al*., 2010) and ATM being essential in *Saccharomyces cerevisiae* (Brush *et al*., 1996). *ATR* may either be not essential in the BSF, or simply not depleted sufficiently to have an effect.

As the BSF *ATM* RNAi clones that showed an RNAi-associated growth phenotype have been studied in much more detail the most pressing next step should be to bring the remainder of the RNAi cell lines in both BSF and PCF to a similar point. In particular the BSF *ATM* RNAi clones which didn't show a response to tetracycline should be examined for any knockdown to determine whether they have a different level of knockdown or no knockdown at all, and the levels of knockdown in the PCF and BSF *ATR* cell lines should be established to establish the relevance (or otherwise) of their growth phenotypes shown so far. If knockdowns can be confirmed they should provide a good platform for examining DNA damage functions. In particular the MMS experiment should be continued in the PCF parasites. As these cell lines do not have a lethal phenotype it should be easier to distinguish between effects that are due purely to the RNAi and effects caused by the MMS in a potentially DNA damage response impaired cell line.

It is not clear why the northern blots failed to show a clear band for *ATM* and *ATR*. Given the smears it is likely that this is due to degradation of the RNA, but all appropriate precautions for working with RNA were taken. Additionally, the tubulin control demonstrated that at least some of the mRNA in the preparation was intact. It is possible that the large predicted size of the *ATM* and *ATR* mRNAs makes them particularly susceptible to degradation.

The RNAi cell lines may provide a way to probe for a connection between the DNA damage response pathways and antigenic variation. It has already been shown that DSBs are involved in this process (Boothroyd *et al*., 2009) and so are several DNA damage response proteins such as BRCA2 (Hartley and McCulloch, 2008b) and Rad51 and its paralogues (Dobson *et al*., 2011), so it may be that at least ATM and perhaps ATR are also involved. It would probably be impossible to use the *ATM* RNAi cell lines to examine this link due to the quickly lethal phenotype. If the BSF *ATR* RNAi cell lines do show a knockdown, however, then it should be possible to examine switching rates during induction as there is no growth phenotype for these cell lines. Alternatively it may be possible to produce single knockout cell lines of ATM, which if they show a less extreme phenotype may be able to address this question.

Single knockout cell lines should be attempted for both *ATM* and *ATR* in order to test that the functions of the natively tagged proteins are not affected adversely by the addition of the tags. This would then allow confidence in the use of the tagged proteins to look for localisation of ATM and ATR before and after DNA damage, and look for colocalisation with other DNA damage response proteins, such as Rad51 and Mre11. Double knockouts would then be a sensible next step, particularly in the PCF, assuming that neither of these proteins is essential there. This may allow the use of the PCF to look for general functions of these proteins in trypanosomes, which could be extrapolated to the BSF.

In summary, this project has developed a technique to assist in cell cycle related analysis and taken some steps to use this technique to search for links between the cell cycle and DNA damage response proteins. Analysis of two specific DNA damage response signalling proteins, ATM and ATR, has been initiated and further work to complete this would allow analysis of the link these proteins are hypothesised to possess in *T. brucei* to the DNA damage response and the cell cycle, and from these further possible links to antigenic variation. Alternatively, lack of function in the DNA damage response would

suggest that *T*. b*rucei* possesses an unusual system of control for its DNA damage response system compared to the more highly studied eukaryotic organisms.

Bibliography

Abraham,R.T. (2004) PI 3-kinase related kinases: `big' players in stress-induced signaling pathways, DNA Repair, vol.3: pp883-887

Agarwal,S., Tafel,AA, and Kanaar,R (2006) DNA double-strand break repair and chromosome translocations, DNA Repair, vol.5: pp1075-1081

Allen, J.B., Zhou, Z., Siede, W., Friedberg, E.C., and Elledge, S.J. (1994) The Sad1/Rad53 protein kinase controls multiple checkpoints and DNA damage-induced transcription in yeast, Genes And Development, vol.8: pp2401-2415

Ali,A., Zhang,J, Bao,S, Liu,I, Otterness,D, Dean,NM, Abraham,RT, and Wang,XF (2004) Requirement of protein phosphatase 5 in DNA-damage-induced ATM activation, Genes and Development, vol.18: pp249-254

Ambit,A. (2006) Characterisation of *Leishmania major* metacaspase, pp50-56, PhD Thesis in: Wellcome Trust Centre for Molecular Parasitology, University of Glasgow, Glasgow, UK

Aparicio,O.M., Stout,AM, and Bell,SP (1999) Differential assembly of Cdc45p and DNA polymerases at early and late origins of DNA replication, Proceedings of the National Academy of Sciences of the United States of America, vol.96: pp9130-9135

Archer,S.K., Inchaustegui,D, Queiroz,R, and Clayton,C (2011) The Cell Cycle Regulated Transcriptome of *Trypanosoma brucei*, PLoS ONE, vol.6: ppe18425-

Bakkenist,C.J. and Kastan,MB (2003) DNA damage activates ATM through intermolecular autophosphorylation and dimer dissociation, Nature, vol.421: pp499-506

Barzel,A. and Kupiec,M (2008) Finding a match: how do homologous sequences get together for recombination?, Nat Rev Genet, vol.9: pp27-37

Bekker-Jensen,S. and Mailand,N (2010) Assembly and function of DNA double-strand break repair foci in mammalian cells, DNA Repair, vol.9: pp1219-1228

Birkett,C.R., Foster,KE, Johnson,L, and Gull,K (1985) Use of monoclonal antibodies to analyse the expression of a multi-tubulin family, FEBS Letters, vol.187: pp211-218

Boothroyd,C.E., Dreesen,O, Leonova,T, Ly,KI, Figueiredo,LM, Cross,GAM, and Papavasiliou,FN (2009) A yeast-endonuclease-generated DNA break induces antigenic switching in *Trypanosoma brucei*, Nature, vol.459: pp278-281

Bringaud,F., Rivi□re,L, and Coustou,V (2006) Energy metabolism of trypanosomatids: Adaptation to available carbon sources, Molecular and Biochemical Parasitology, vol.149: pp1-9

Brown,E.J. and Baltimore,D (2000) ATR disruption leads to chromosomal fragmentation and early embryonic lethality, Genes & Development, vol.14: pp397-402

Brush,G., Morrow,D, Hieter,P, and Kelly,T (1996) The ATM homologue MEC1 is required for phosphorylation of replication protein A in□Çëyeast, Proceedings of the National Academy of Sciences, vol.93: pp15075-15080

Burton,P., McBride,DJ, Wilkes,JM, Barry,JD, and McCulloch,R (2007) Ku heterodimer-independent end joining in *Trypanosoma brucei* cell extracts relies upon sequence microhomology, Eukaryotic Cell, vol.6: pp1773-1781

Cahill,D., Connor,B, and Carney,J (2006) Mechanisms of eukaryotic DNA double strand break repair, Frontiers in Bioscience, vol.11: pp1958-1976

Carrington,M., Miller,N, Blum,M, Roditi,I, Wiley,D, and Turner,M (1991) Variant specific glycoprotein of *Trypanosoma brucei* consists of two domains each having an independently conserved pattern of cysteine residues, Journal of Molecular Biology, vol.221: pp823-835

Center for Disease Control (2010) Parasites - African Trypanosomiasis (http://www.cdc.gov/parasites/sleepingsickness/)

Chen,G., Yuan,SS, Liu,W, Xu,Y, Trujillo,K, Song,B, Cong,F, Goff,SP, Wu,Y, Arlinghaus,R, Baltimore,D, Gasser,PJ, Park,MS, Sung,P, and Lee,EYH (1999) Radiation-induced Assembly of Rad51 and Rad52 Recombination Complex Requires ATM and c-Abl, Journal of Biological Chemistry, vol.274: pp12748-12752

Chowdhury,A.R., Zhao,Z, and Englund,PT (2008) Effect of Hydroxyurea on Procyclic Trypanosoma brucei: an Unconventional Mechanism for Achieving Synchronous Growth, Eukaryotic Cell, vol.7: pp425-428

Chun,H.H. and Gatti,RA (2004) Ataxia-telangiectasia, an evolving phenotype, DNA Repair, vol.3: pp1187-1196

Cook,J.G. (2009) Replication licensing and the DNA damage checkpoint, Frontiers in Bioscience, vol.14: pp5013-5030

D'Amours,D. and Jackson,SP (2002) The MRE11 complex: at the crossroads of DNA repair and checkpoint signalling, Nature Review Molecular and Cellular Biology, vol.3: pp317-327

de Jager,M., van Noort,J, van Gent,DC, Dekker,C, Kanaar,R, and Wyman,C (2001) Human Rad50/Mre11 Is a flexible complex that can tether DNA ends, Molecular Cell, vol.8: pp1129-1135

De Wulf,P., Montani,F., Visintin,R. (2009) Protein phosphatases take the mitotic stage, Current Opinion in Cell Biology, vol.21(6): pp806-815

Derheimer,F.A. and Kastan,MB (2010) Multiple roles of ATM in monitoring and maintaining DNA integrity, FEBS Letters, vol.584: pp3675-3681

Dobson,R. (2009) Analysis of the functions and interactions of the RAD51 paralogues in *Trypanosoma brucei*, pp36-41, 67-254, PhD Thesis in: Wellcome Trust Centre for Molecular Parasitology, University of Glasgow, Glasgow, UK

Dobson,R., Stockdale,C, Lapsley,C, Wilkes,J, and McCulloch,R (2011) Interactions among Trypanosoma brucei RAD51 paralogues in DNA repair and antigenic variation, Molecular Microbiology, vol:81(2) pp434-56

Dubrana,K., van Attikum,H, Hediger,F, and Gasser,SM (2007) The processing of double-strand breaks and binding of single-strand-binding proteins RPA and Rad51 modulate the formation of ATR-kinase foci in yeast, Journal of Cell Science, vol.120: pp4209-4220

Earnshaw,W.C. and Laemmli,UK (1983) Architecture of Metaphase Chromosomes and Chromosome Scaffolds, Journal of Cell Biology, vol.96: pp84-93

Ellison,V. and Stillman,B (2003) Biochemical characterization of DNA damage checkpoint complexes: clamp loader and clamp complexes with specificity for 5' recessed DNA, PLoS.Biol, vol.1: ppE33-

Fenn,K. and Matthews,KR (2007) The cell biology of *Trypanosoma brucei* differentiation, Current Opinion in Microbiology, vol.10: pp539-546

Forsythe,G.R., McCulloch,R, and Hammarton,TC (2009) Hydroxyurea-induced synchronisation of bloodstream stage *Trypanosoma brucei*, Molecular and Biochemical Parasitology, vol.164: pp131-136

Gilad,O., Nabet,BY, Ragland,RL, Schoppy,DW, Smith,KD, Durham,AC, and Brown,EJ (2010) Combining ATR suppression with oncogenic Ras synergistically increases genomic instability, causing synthetic lethality or tumorigenesis in a dosage-dependent manner, Cancer Research, vol.70: pp9693-9702

Glover,L., Jun,J, and Horn,D (2011) Microhomology-mediated deletion and gene conversion in African trypanosomes, Nucleic Acids Research, vol.39: pp1372-1380

Glover,L., McCulloch,R, and Horn,D (2008) Sequence homology and microhomology dominate chromosomal double-strand break repair in African trypanosomes, Nucleic Acids Research, vol.36: pp2608-2618

Glynn,M., Kaczmarczyk,A, Prendergast,L, Quinn,N, and Sullivan,KF (2010) Centromeres: assembling and propagating epigenetic function, vol.50: pp223-249

Goodarzi,A.A., Jonnalagadda,JC, Douglas,P, Young,D, Ye,R, Moorhead,GBG, Lees-Miller,SP, and Khanna,KK (2007) Autophosphorylation of ataxia-telangiectasia mutated is regulated by protein phosphatase 2A, EMBO, vol.23: pp4451-4461

Grallert,B. and Boye,E (2008) The multiple facets of the intra-S checkpoint, Cell Cycle, vol.7: pp2315-2320

Gudmundsdottir,K. and Ashworth,A (2006) The roles of BRCA1 and BRCA2 and associated proteins in the maintenance of genomic stability, Oncogene, vol.25: pp5864-5874

Haber,J.E. (1998) The Many Interfaces of Mre11, Cell, vol.95: pp583-586

Hall-Jackson,C.A., Cross,DAE, Morrice,N, and Smythe,C (1999) ATR is a caffeine-sensitive, DNA-activated protein kinase with a substrate specificity distinct from DNA-PK, Oncogene, vol.18: pp6707-6713

Hammarton,T.C. (2007) Cell cycle regulation in *Trypanosoma brucei*, Molecular and Biochemical Parasitology, vol.153: pp1-8

Hammarton,T.C., Monnerat,S, and Mottram,JC (2007) Cytokinesis in trypanosomatids, Current Opinion in Microbiology, vol.10: pp520-527

Harrison,J.C. and Haber,JE (2006) Surviving the breakup: the DNA damage checkpoint, Annual Review of Genetics, vol.40: pp209-235

Hartley,C.L. and McCulloch,R (2008a) Trypanosoma brucei BRCA2 acts in antigenic variation and has undergone a recent expansion in BRC repeat number that is important during homologous recombination, Molecular Microbiology, vol.68: pp1237-1251

Hartley,C.L. and McCulloch,R (2008b) Trypanosoma brucei BRCA2 acts in antigenic variation and has undergone a recent expansion in BRC repeat number that is important during homologous recombination, Molecular Microbiology, vol.68: pp1237-1251

Harvey,S.H., Sheedy,DM, Cuddihy,AR, and O'Connell,MJ (2004) Coordination of DNA damage responses via the Smc5/Smc6 complex, Molecular and Cellular Biology, vol.24: pp662-674

Horn,D. and McCulloch,R (2010) Molecular mechanisms underlying the control of antigenic variation in African trypanosomes, Current Opinion in Microbiology, vol.13: pp700-705

Jaberaboansari,A., Nelson,GB, Roti,JLR, and Wheeler,KT (1988) Postirradiation alterations of neuronal chromatin structure, Radiation Research, vol.114: pp94-104

Kabani,S., Waterfall,M, and Matthews,KR (2010) Cell-cycle synchronisation of bloodstream forms of *Trypanosoma bruce*i using Vybrant DyeCycle Violet-based sorting, Molecular and Biochemical Parasitology, vol.169: pp59-62

Kanu,N. and Behrens,A (2008) ATMINistrating ATM signalling: regulation of ATM by ATMIN, Cell Cycle, vol.7: pp3483-3486

Kieft,R., Capewell,P, Turner,CM, Veitch,NJ, MacLeod,A, and Hajduk,S (2010) Mechanism of *Trypanosoma brucei gambiense* (group 1) resistance to human trypanosome lytic factor, Proceedings of the National Academy of Sciences, vol.107: pp16137-16141

Kiyokawa,H. and Ray,D (2008) In Vivo Roles of CDC25 Phosphatases: Biological insight into the anti-cancer therapeutic targets, Anti-Cancer Agents in Medicinal Chemistry, vol.8: pp832-836

Krajewski,W.A. (1995) Alterations in the internucleosomal DNA helical twist in chromatin of human erythroleukemia-cells *in-vivo* influences the chromatin higher-order folding, FEBS Letters, vol.361: pp149-152

LaCount,D.J., Bruse,S, Hill,KL, and Donelson,JE (2000) Double-stranded RNA interference in *Trypanosoma brucei* using head-to-head promoters, Molecular and Biochemical Parasitology, vol.111: pp67-76

Lee,A.Y.-L., Liu,E, and Wu,X (2007) The Mre11/Rad50/Nbs1 Complex plays an important role in the prevention of DNA rereplication in mammalian cells, Journal of Biological Chemistry, vol.282: pp32243-32255

Lee,W.C., Bhagat,AA, Huang,S, Van Vliet,KJ, Han,J, and Lim,CT (2011) High-throughput cell cycle synchronization using inertial forces in spiral microchannels, Lab on a Chip, vol.11: pp1359-1367

Liermann,B., Lassmann,G, and Langen,P (1990) Quenching of tyrosine radicals of M2 subunit from ribonucleotide reductase in tumor cells by different antitumor agents: An EPR study, Free Radical Biology and Medicine, vol.9: pp1-4

Liu,B.Y., Liu,YN, Motyka,SA, Agbo,EEC, and Englund,PT (2005) Fellowship of the rings: the replication of kinetoplast DNA, Trends in Parasitology, vol.21: pp363-369

Lo,T., Pellegrini,L, Venkitaraman,AR, and Blundell,TL (2003) Sequence fingerprints in BRCA2 and RAD51: implications for DNA repair and cancer, DNA Repair, vol.2: pp1015-1028

Lopez-Contreras,A.J. and Fernandez-Capetillo,O (2010) The ATR barrier to replication-born DNA damage, DNA Repair, vol.9: pp1249-1255

Lukas,C., Falck,J, Bartkova,J, Bartek,J, and Lukas,J (2003) Distinct spatiotemporal dynamics of mammalian checkpoint regulators induced by DNA damage, Nature Cell Biology, vol.5: pp255-260

Lundin,C., North,M, Erixon,K, Walters,K, Jenssen,D, Goldman,ASH, and Helleday,T (2005) Methyl methanesulfonate (MMS) produces heat-labile DNA damage but no detectable in vivo DNA double-strand breaks, Nucleic Acids Research, vol.33: pp3799-3811

Marcello,L. and Barry,JD (2007) Analysis of the VSG gene silent archive in *Trypanosoma brucei* reveals that mosaic gene expression is prominent in antigenic variation and is favored by archive substructure, Genome Research, vol.17: pp1344-1352

Matsuoka,S., Ballif,BA, Smogorzewska,A, McDonald,ER, III, Hurov,KE, Luo,J, Bakalarski,CE, Zhao,Z, Solimini,N, Lerenthal,Y, Shiloh,Y, Gygi,SP, and Elledge,SJ (2007) ATM and ATR substrate analysis reveals extensive protein networks responsive to DNA damage, Science, vol.316: pp1160-1166

McCulloch,R. and Barry,JD (1999) A role for RAD51 and homologous recombination in *Trypanosoma brucei* antigenic variation, Genes and Development, vol.13: pp2875-2888

McIlwraith,M.J., Vaisman,A, Liu,Y, Fanning,E, Woodgate,R, and West,SC (2005) Human DNA polymerase [eta] promotes DNA synthesis from strand invasion intermediates of homologous recombination, Molecular Cell, vol.20: pp783-792

McKean,P.G., Keen,JK, Smith,DF, and Benson,FE (2001) Identification and characterisation of a RAD51 gene from *Leishmania major*, Molecular and Biochemical Parasitology, vol.115: pp209-216

Misri,S., Pandita,S, Kumar,R, and Pandita,TK (2008) Telomeres, histone code, and DNA damage response, Cytogenetic and Genome Research, vol.122: pp297-307

Munday,J.C., McLuskey,K., Brown,E., Coombs,G.H., and Mottram,J.C. (2011) Oligopeptidase B deficient mutants of Leishmania major Molecular and Biochemical Parasitology, vol.175: pp49-57.

Mutomba,M.C. and Wang,CC (1996) Effects of aphidicolin and hydroxyurea on the cell cycle and differentiation of *Trypanosoma brucei* bloodstream forms, Molecular and Biochemical Parasitology, vol.80: pp89-102

Ogawa,T., Yu,X, Shinohara,A, and Egelman,EH (1993) Similarity of the yeast Rad51 filament to the bacterial RecA filament, Science, vol.259: pp1896-1899

Olson,E., Nievera,CJ, Liu,E, Lee,AY-L, Chen,L, and Wu,X (2007) The Mre11 complex mediates the S-phase checkpoint through an interaction with Replication Protein A, Molecular and Cellular Biology, vol.27: pp6053-6067

Ouchi,T., Monteiro,AN, August,A, Aaronson,SA, and Hanafusa,H (1998) BRCA1 regulates p53-dependent gene expression, Proceedings of the National Academy of Sciences, vol.95: pp2302-2306

Parsons,M., Worthey,E, Ward,P, and Mottram,J (2005) Comparative analysis of the kinomes of three pathogenic trypanosomatids: *Leishmania major*, *Trypanosoma brucei* and *Trypanosoma cruzi*., BMC Genomics, vol.6: pp127-142

Proudfoot,C. and McCulloch,R (2005) Distinct roles for two RAD51-related genes in *Trypanosoma brucei* antigenic variation, Nucleic Acids Research, vol.33: pp6906-6919

Proudfoot,C. and McCulloch,R (2006) *Trypanosoma brucei* DMC1 does not act in DNA recombination, repair or antigenic variation in bloodstream stage cells, Molecular and Biochemical Parasitology, vol.145: pp245-253

Regis-Da-Silva,C.G., Freitas,JM, Passos-Silva,DG, Furtado,C, Augusto-Pinto,L, Pereira,MT, DaRocha,WD, Franco,GR, Macedo,AM, Hoffmann,JS, Cazaux,C, Pena,SDJ, Teixeira,SMR, and Machado,CR (2006) Characterization of the *Trypanosoma cruzi* Rad51 gene and its role in recombination events associated with the parasite resistance to ionizing radiation, Molecular and Biochemical Parasitology, vol.149: pp191-200

Robinson,N.P., McCulloch,R, Conway,C, Browitt,A, and Barry,JD (2002) Inactivation of Mre11 does not affect VSG gene duplication mediated by homologous recombination in *Trypanosoma brucei*, Journal of Biological Chemistry, vol.277: pp26185-26193

Rout,M.P. and Field,MC (2001) Isolation and characterization of subnuclear compartments from *Trypanosoma brucei* - Identification of a major repetitive nuclear lamina component, Journal of Biological Chemistry, vol.276: pp38261-38271

Rupnik,A., Lowndes,NF, and Grenon,M (2010) MRN and the race to the break, Chromosoma, vol.119: pp115-135

San Filippo,J., Sung,P, and Klein,H (2008) Mechanism of eukaryotic homologous recombination, Annual Review of Biochemistry, vol.77: pp229-257

Schar,P., Fasi,M, and Jessberger,R (2004) SMC1 coordinates DNA double-strand break repair pathways, Nucleic Acids Research, vol.32: pp3921-3929

Schneider,A., Bursac,D, and Lithgow,T (2008) The direct route: a simplified pathway for protein import into the mitochondrion of trypanosomes, Trends in Cell Biology, vol.18: pp12-18

Schorl,C. and Sedivy,JM (2007) Analysis of cell cycle phases and progression in cultured mammalian cells, Methods, vol.41: pp143-150

Shechter,D., Costanzo,V, and Gautier,J (2004) ATR and ATM regulate the timing of DNA replication origin firing, Nature Cell Biology, vol.6: pp648-655

Shiloh,Y. (2001) ATM and ATR: networking cellular responses to DNA damage, Current Opinion in Genetics & Development, vol.11: pp71-77

Shiloh,Y. (2003) ATM and related protein kinases: safeguarding genome integrity, Nature Review Cancer, vol.3: pp155-168

Siegel, T.N., Hekstra, D.R., Cross, G.A.M. (2008) Analysis of the *Trypanosoma brucei* cell cycle by quantitative DAPI imaging, Molecular and Biochemical Parasitology, vol.160: pp171–174

Smith,C.E., Llorente,B, and Symington,LS (2007) Template switching during break-induced replication, Nature, vol.447: pp102-105

So,S., Davis,AJ, and Chen,DJ (2009) Autophosphorylation at serine 1981 stabilizes ATM at DNA damage sites, The Journal of Cell Biology, vol.187: pp977-990

Soutoglou,E. and Misteli,T (2008) Activation of the cellular DNA damage response in the absence of DNA lesions, Science, vol.320: pp1507-1510

Sugiyama,T., Kantake,N, Wu,Y, and Kowalczykowski,SC (2006) Rad52-mediated DNA annealing after Rad51-mediated DNA strand exchange promotes second ssDNA capture, Embo Journal, vol.25: pp5539-5548

Sun,Y., Jiang,X, and Price,BD (2010) Tip60: Connecting chromatin to DNA damage signaling, Cell Cycle, vol.9: pp930-936

Sung,P. and Klein,H (2006) Mechanism of homologous recombination: mediators and helicases take on regulatory functions, Nature Reviews Molecular Cell Biology, vol.7: pp739-750

Suzuki,K., Okada,H, Yamauchi,M, Oka,Y, Kodama,S, and Watanabe,M (2006) Qualitative and quantitative analysis of phosphorylated ATM foci induced by low-dose ionizing radiation, Radiation Research, vol.165: pp499-504

Trenz,K., Smith,E, Smith,S, and Costanzo,V (2006) ATM and ATR promote Mre11 dependent restart of collapsed replication forks and prevent accumulation of DNA breaks, EMBO J, vol.25: pp1764-1774

Truong,L.N. and Wu,X (2011) Prevention of DNA re-replication in eukaryotic cells, Journal of Molecular Cell Biology, vol.3: pp13-22

Valero,A., Braschler,T, Rauch,A, Demierre,N, Barral,Y, and Renaud,P (2011) Tracking and synchronization of the yeast cell cycle using dielectrophoretic opacity, Lab on a Chip, vol.11: pp1754-1760

van Hellemond,J.J., Opperdoes,FR, and Tielens,AGM (2005) The extraordinary mitochondrion and unusual citric acid cycle in *Trypanosoma brucei*, Biochemical Society Transactions, vol.33: pp967-971

Vanhamme,L., Paturiaux-Hanocq,F, Poelvoorde,P, Nolan,DP, Lins,L, Van Den Abbeele,J, Pays,A, Tebabi,P, Van Xong,H, Jacquet,A, Moguilevsky,N, Dieu,M, Kane,JP, De Baetselier,P, Brasseur,R, and Pays,E (2003) Apolipoprotein L-I is the trypanosome lytic factor of human serum, Nature, vol.422: pp83-87

Vassilev,A., Yamauchi,J, Kotani,T, Prives,C, Avantaggiati,ML, Qin,J, and Nakatani,Y (1998) The 400 kDa Subunit of the PCAF histone acetylase complex belongs to the *ATM* superfamily, Molecular Cell, vol.2: pp869-875

Vendelbo,M.H. and Nair,KS (2011) Mitochondrial longevity pathways, Biochimica et Biophysica Acta (BBA) - Molecular Cell Research, vol.1813: pp634-644

Vickerman,K. (1985) Developmental cycles and biology of pathogenic trypanosomes, British Medical Bulletin, vol.41: pp105-114

Ward,I.M. and Chen,J (2001) Histone H2AX is phosphorylated in an ATR-dependent manner in response to replicational stress, Journal of Biological Chemistry, vol.276: pp47759-47762

Wheeler,R.J. (2010) The trypanolytic factor-mechanism, impacts and applications, Trends in Parasitology, vol.26: pp457-464

WHO (2010) African trypanosomiasis (sleeping sickness),

Wirtz,E., Leal,S, Ochatt,C, and Cross,GAM (1999) A tightly regulated inducible expression system for conditional gene knock-outs and dominant-negative genetics in *Trypanosoma brucei*, Molecular and Biochemical Parasitology, vol.99: pp89-101

Wong,A.K.C., Pero,R, Ormonde,PA, Tavtigian,SV, and Bartel,PL (1997) RAD51 Interacts with the evolutionarily conserved BRC motifs in the human breast cancer susceptibility gene BRCA2, Journal of Biological Chemistry, vol.272: pp31941-31944

Woodward,R. and Gull,K (1990) Timing of nuclear and kinetoplast DNA replication and early morphological events in the cell cycle of *Trypanosoma brucei,* Journal of Cell Science, vol.95: pp49-57

Xu,B., Kim,St, and Kastan,MB (2001) Involvement of BRCA1 in S-Phase and G2-Phase checkpoints after ionizing irradiation, Molecular and Cellular Biology, vol.21: pp3445-3450

Yazdi,P.T., Wang,Y, Zhao,S, Patel,N, Lee,EYH, and Qin,J (2002) SMC1 is a downstream effector in the ATM/NBS1 branch of the human S-phase checkpoint, Genes and Development, vol.16: pp571-582

Zou,L. and Elledge,SJ (2003) Sensing DNA damage through ATRIP recognition of RPA-ssDNA Complexes, Science, vol.300: pp1542-1548